OCEAN, ICE, AND ATMOSPHERE: INTERACTIONS AT THE ANTARCTIC CONTINENTAL MARGIN
ANTARCTIC RESEARCH SERIES, VOLUME 75, PAGES 215-240

WESTERN WEDDELL SEA THERMOHALINE STRATIFICATION

Arnold L. Gordon

Lamont-Doherty Earth Observatory of Columbia University

The United States - Russian Ice Station Weddell expedition of February to June 1992 provided a detailed view of the circulation and stratification of the western Weddell Sea. There a narrow band of the warmest Weddell Deep Water, which comprises the bulk of the water column, is advected along the western boundary current axis and underlain by a very cold, highly oxygenated benthic layer. Within that layer, at some locations, a low salinity variety of Weddell Sea Bottom Water is displaced upward by more saline bottom water. The low salinity type is primarily introduced into the deep ocean immediately west of General Belgrano Bank and incorporates Ice Shelf Water from the Ronne Ice Shelf. It snakes northward near the 3000 m isobath, descending to depths >4000 m near 65°S, 50°W to feed the eastward-flowing northern limb of the Weddell Gyre. The saline type comes from High Salinity Shelf Water that descends into the deep ocean at a number of sites along the western shelf. Thermohaline and oxygen properties within the benthic layer differ little from shelf waters, indicating minor mixing between slope plumes and Weddell Deep Water. The high salinity bottom water is dense enough to have reached the sea floor without thermobaric effects, but the low salinity variety must first attain a depth of ≈500-800 dbar. The average salinity of the benthic layer is too low to provide for the cold end-member mixing component within Weddell Gyre deep water. This suggests that recent bottom water formation is less saline, containing more glacial ice meltwater than in past decades. The total Weddell Sea Bottom Water (<-0.7°C) formation rate is estimated to be 4.0-4.8 Sv for the February - June 1992 period. A trough in the main pycnocline over the upper slope, associated with the Antarctic Slope Front, represents a convergence zone dividing the continental margin from open ocean contributions to deep reaching convection. On its seaward side sinking occurs into the deep water, and on its shoreward side the denser surface water penetrates to the sea floor. Within the axis and somewhat seaward of the pycnocline trough, a relatively cold, low salinity layer, containing glacial meltwater from the southeastern Weddell Sea, forms the upper part of the pycnocline. The resulting increased upper water column stability, the greater depth of the warm core in this sector and the absence of strong mixing inhibits vertical heat flux in the western Weddell Sea, contributing to its perennial sea cover.

1. INTRODUCTION

The Weddell Gyre is the largest of the cyclonic gyres occupying the region between the Antarctic Circumpolar Current (ACC) and Antarctica, stretching from the Antarctic Peninsula to 30°E. Its unique environmental setting allows water of abyssal ocean density to have nearly isopycnal communication with the surface ocean, sea ice, glacial ice and cold polar atmosphere. The ensuing sea-air-ice heat and freshwater fluxes lead to the formation of the coldest, densest ocean water masses of global importance:Weddell Sea Bottom Water (WSBW),

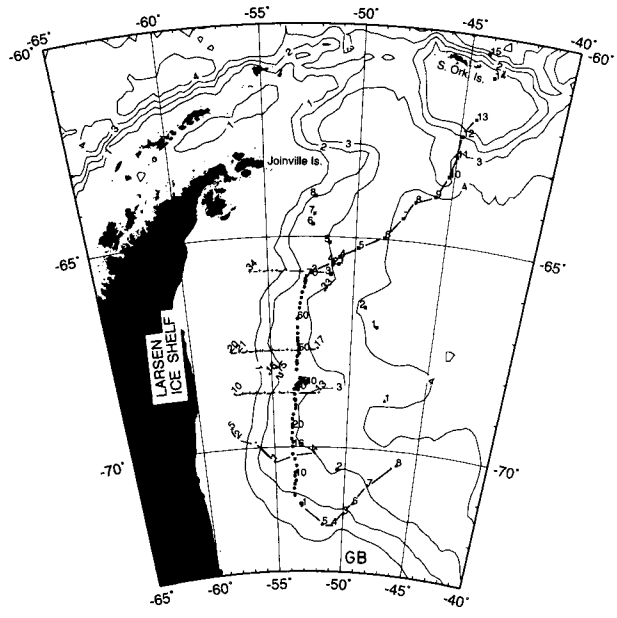

Fig. 1. Conductivity-temperature-depth (CTD) stations occupied during the Ice Station Weddell [*Huber et al.*, 1994] project. Casts from the Ice Station are shown as dots, from the helicopter as plusses, from the *Federov* as triangles, and from the *Palmer* as solid boxes. The lines connecting individual stations locate the sections displayed in Figures 5 to 9, including *Palmer* cruises 92-2. *Palmer* cruise 92-1 stations are unconnected. The bottom bathymetry (1, 2, 3, and 4 km isobaths) are taken from *LaBrecque and Ghidella* [1993]. GB stands for General Belgrano Bank.

which in a more dilute form is called Antarctic Bottom Water (AABW).

Deacon [1937, 1979] provides important historical perspective on this region. The excellent papers of *Gill* [1973], *Carmack and Foster* [1975a,b] and *Foster and Carmack* [1976a,b] mark the beginning of the modern era of Weddell Sea physical oceanographic research, as does *Weiss et al.* [1979] for chemical and tracer oceanography. In more recent years many useful studies have described the Weddell Gyre stratification and circulation. *Fahrbach et al.* [1998] provide a comprehensive summary of Weddell circulation and water masses. *Orsi et al.* [1993] discuss Weddell Gyre water masses based on isopycnal analysis, while *Mensch et al.* [1996; this volume] and *Weppernig et al.* [1996] bring the added dimension of tracer chemistry to water mass origin and residence time studies. *Gouretski and Danilov* [1993] detail features of the Gyre's eastern boundary. *Fahrbach et al.* [1994a; 1995] and *Muench and Gordon* [1995] discuss the circulation and water masses of the western boundary current, south of a line connecting Joinville Island (Figure 1) to Kapp Norvegia (71°20'S; 11°40'W), forming the western embayment of the Weddell Gyre. *Gammelsrød et al.* [1994] focus on the continental shelf water masses. *Gordon and Huber* [1990; 1995] and *McPhee et al.* [1996] discuss the relatively large vertical heat flux between the surface and deep water within the interior Weddell Gyre. *Martinson* [1990], *Akitomo et al.* [1995] and *Alverson and Owens* [1996] present models of vertical fluxes and convection within that region, while *Robertson et al.* [1995] and *Lytle and Ackley* [1996] consider vertical heat fluxes in the western Weddell Sea. *Robertson et al.* [this volume] model the Weddell Sea tidal currents. *Foster and Middleton* [1984], *Muench et al.* [1990a,b; 1992], *Locarnini et al.* [1993] and *Whitworth et al.* [1994] discuss the oceanographic regime of the northwest Weddell Sea and its interaction with the Scotia Sea at the Weddell-Scotia Confluence.

The objective of this study is to present a detailed overview of the thermohaline stratification and inferred circulation of the western edge of the Weddell Sea. This work was made possible by the collection of an extensive array of oceanographic observations during the United States - Russian Ice Station Weddell project of 1992 [ISW Group 1993; Figure 1]. Sections 2 and 3 present the sea surface relief of the Weddell Gyre relative to 1000 decibar (dbar) and the background to the Weddell Ice Station Expedition. Section 4 provides the basic Ice Station Weddell physical oceanographic data in profile, section and potential temperature versus salinity (θ/S) format. Section 5 discusses various aspects of the circulation, convection and water mass structure, and the global importance of Weddell Sea Bottom Water. Section 6 lists the major conclusions of this study.

2. WEDDELL GYRE CIRCULATION

The dynamic height of the sea surface relative to 1000 dbar pressure provides a view of the baroclinic surface circulation pattern of the Weddell Gyre (Figure 2). Baroclinic shear within the interior of the gyre is small, typically less than 2 cm s^{-1}, reaching 4 cm s^{-1} over Maud Rise. *Muench and Gordon* [1995] reported higher shear of about 6 cm s^{-1} over the continental shelf break and upper slope in the western sector. A characteristic of the continental margin is that geostrophic flow of the sea surface relative to an assumed zero flow at the sea floor is opposite in direction to the surface current observed by iceberg and buoy drift [*Tchernia and Jeannin*, 1983; *Ackley and Holt*, 1984; *Barber and*

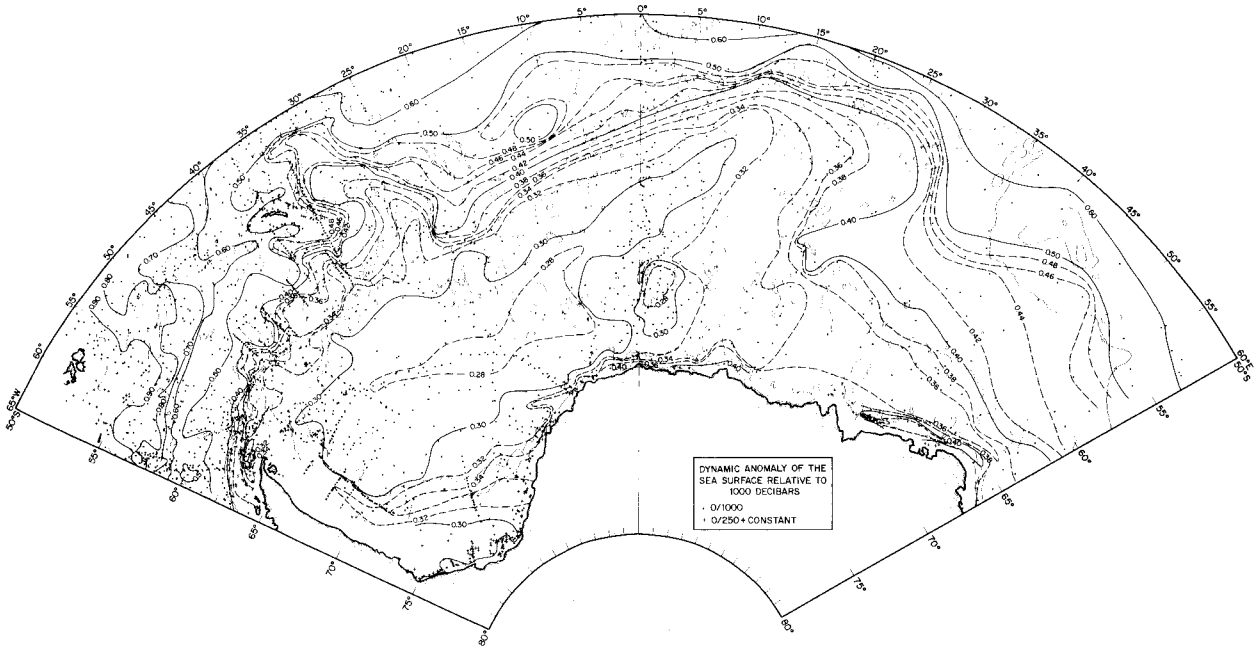

Fig. 2. Height of the sea surface of the Weddell Gyre relative to the 1000 decibar (dbar) pressure surface, in dynamic meters, for an ocean of 0°C and 35 psu in salinity. For areas with depths <1000 dbar, the surface values relative to 250 dbar are added to the regional average 250 relative to 1000 dbar value. Station control, including the data from Figure 1, is shown as dots along with the 2000 m and 3000 m isobaths. Maud Rise is the seamount centered at 65°S, 30°E; Kapp Norvegia is the coastal feature near 12°W.

Crane, 1995] and by direct current measurements [*Muench and Gordon*, 1995; *Fahrbach et al.*, 1992, 1994a]. *Muench and Gordon* [1995] found that the strongest northward geostrophic current (10 - 13 cm s^{-1}) relative to near surface currents occurred at the sea floor within the very cold benthic layer. *Hollister and Elder* [1969] inferred strong northward bottom currents in the western Weddell from a study of compass oriented sea floor photographs. *Heywood et al.* [1997] determined a baroclinic (referenced to the sea floor) westward transport of a 4 Sv (1 Sv $\equiv 10^6$ m^3s^{-1}) for the eastern Weddell continental slope current across 17°W, but this value rose to 14 Sv when hull mounted Acoustic Doppler Current Profiler data were employed for geostrophic reference. Clearly an assumed zero velocity layer at the sea floor is not a legitimate reference for circulation along the continental margin.

Strong bottom currents associated with narrow boundary currents over steep topography are evident in other long-term measurements. *Bersch et al.* [1992] measured bottom speeds of 1.5 to 5.2 cm s^{-1} over the flanks of Maud Rise. *Fahrbach et al.* [1992] reported average westward bottom speeds of 2 - 6 cm s^{-1} over the shelf and slope near Kapp Norvegia, with higher values at ≈670 m near the shelf break, and currents of 3 to nearly 7 cm s^{-1} adjacent to Vestkapp (near 20°W). *Foldvik et al.* [1985a] measured bottom flow of 6 to 7 cm s^{-1} 100 m above the 630 m sea floor, associated with a dense plume emanating from the mouth of the Filchner Depression [*Foldvik et al.*, 1985b]. *Barber and Crane* [1995] measured bottom flow of 7 to 11 cm s^{-1} in about 4000 m of water near 63.5°S and 42°W where the western boundary current of the Weddell Gyre turns eastward. *Fahrbach et al.* [1994a] found bottom currents of ≈10 cm s^{-1} over the slope adjacent to Joinville Island, but weak bottom velocities over the deep, flat sea floor. Rather than a shear field forced by the wind stress at the sea surface, increasing westward speed with increasing depth may be the consequence of strong buoyancy (thermohaline) forcing along the continental margin, the associated formation of dense water and its escape along the sea floor to the deep ocean. While a deep zero reference level leads to an accurate portrayal of the general pattern of surface circulation over the deep

ocean, a near-zero surface flow may be more appropriate along the Weddell Sea continental margin.

The southern limit of the ACC is defined in its baroclinic mode by closely-spaced isopleths, best represented by the 0.4 dyn m contour between 55° and 60°S, which coincides with the definition of *Orsi et al.* [1995]. South of this ACC limit the Weddell Gyre bulges northward into the eastern Scotia Sea and around South Sandwich Islands, returning southward near 20°W. *Klepikov* [1964] and *Bagriantsev et al.* [1989] speculated that the Weddell Gyre may at times break into eastern and western cells along this meridian. East of the Greenwich Meridian, the Weddell Gyre's northern edge tracks along the mid-ocean ridge. The eastern boundary occurs between 10° and 30°E, where sea surface dynamic height contours are oriented north-south over a distance of nearly 2000 km from 55° to 70°S. Only part of the water flowing poleward along the eastern boundary turns into the Weddell Gyre, as 0.36 - 0.50 dyn m height anomaly isopleths return to the eastward flow.

The broad central trough of the Weddell Gyre, below 0.30 dyn m, extends westward from 10°E, is aligned northeast-southwest, and passes to the north of Maud Rise. A small isolated baroclinic cyclonic cell over Maud Rise [*Bersch et al.*, 1992], not detected by direct current measurements, may be overwhelmed by opposing topographic controlled barotropic circulation. The relatively rapid rise of sea level as Antarctica is approached marks the westward flowing coastal current, the southern limb of the Weddell Gyre. Over the continental slope (near 1500-m depths) a crest in the baroclinic field extends from the eastern Weddell Sea near 25°W along the western rim of the Weddell Sea. A drop in sea level over the continental shelf denotes an eastward baroclinic flow, but the strong outflow of dense bottom water drives overall flow to the west and north, as noted above and evidenced by Eulerian and Lagrangian current measurements. Because of this effect, the baroclinic field does not clearly reveal the western boundary current of the Weddell Gyre, though its does mark regions where bottom water and not wind stress controls the baroclinic shear.

The 1989 - 1992 observations from Kapp Norvegia to Joinville Island [*Fahrbach et al.* 1994a], showed a Weddell Gyre transport of 29.5 Sv, 90% of which is contained in narrow jets following the continental slope. Using current measurements for geostrophic reference, *Muench and Gordon* [1995] found that western boundary current transport increased from 12 Sv in the southwestern Weddell to about 28 Sv northward across the Ice Station sections. This increase is compensated by westward flow from the interior of the gyre into the western boundary region. About 5-6 Sv of the northward transport, coupled to bottom speeds in excess of 10 cm s^{-1}, is contained within a 300-500 m-thick cold bottom layer of WSBW.

3. ICE STATION WEDDELL

Ice Station Weddell in 1992 was the first intentional scientific Southern Ocean ice drift station. Established in the western Weddell Sea by the joint efforts of the United States and Russia [*ISW Group,* 1993], the station drift followed closely that of the *Endurance* in 1915. Ice Station Weddell was deployed in this largely unexplored corner of the Southern Ocean on 11 February 1992 at 71°48'S, 51°43'W from the *Akademik Fedorov*. After a northward drift of nearly 700 km in 3.5 months, the station was recovered by the *Fedorov* and by the *Nathaniel B. Palmer* on 9 June 1992 at 65°38'S, 52°25'W. Oceanographic data obtained during the project included 137 Conductivity-Temperature-Depth (CTD) profiles [*Huber et al.* 1994] from the Ice Station and its helicopters and from supporting ships. Current meter observations were made from the main camp and from remote sites to define the mean and long period currents [*Muench and Gordon,* 1995] and the higher frequency components [*Levine et al.* 1997]. Microstructure measurements were made to investigate vertical fluxes [*McPhee and Martinson,* 1994; *Robertson et al.*, 1995]. Sea ice thermodynamics and dynamics were studied from in situ and satellite sensors [*Lytle and Ackley,* 1996]. Atmospheric boundary layer measurements defined the wind stress acting on the ice floe [*Andreas and Claffey,* 1995].

4. WESTERN WEDDELL SEA THERMOHALINE STRATIFICATION

4.1 *Profiles*

Deep Ocean. Thermohaline stratification within the deep water column (Figures 3a, 3b) has the basic character of the interior Weddell Gyre. A cold, low salinity surface mixed layer is separated by a rather weak pycnocline, only 0.054 sigma-0 units from 200 m to 350 m on station 35, from a thick layer of warmer, saltier Weddell Deep Water (WDW). The low salinity summer surface layer at station 16, with a sharp seasonal pycnocline at 30 to 50 m, gradually gives way to a more homogeneous surface layer as winter conditions become more fully established during the ice floe

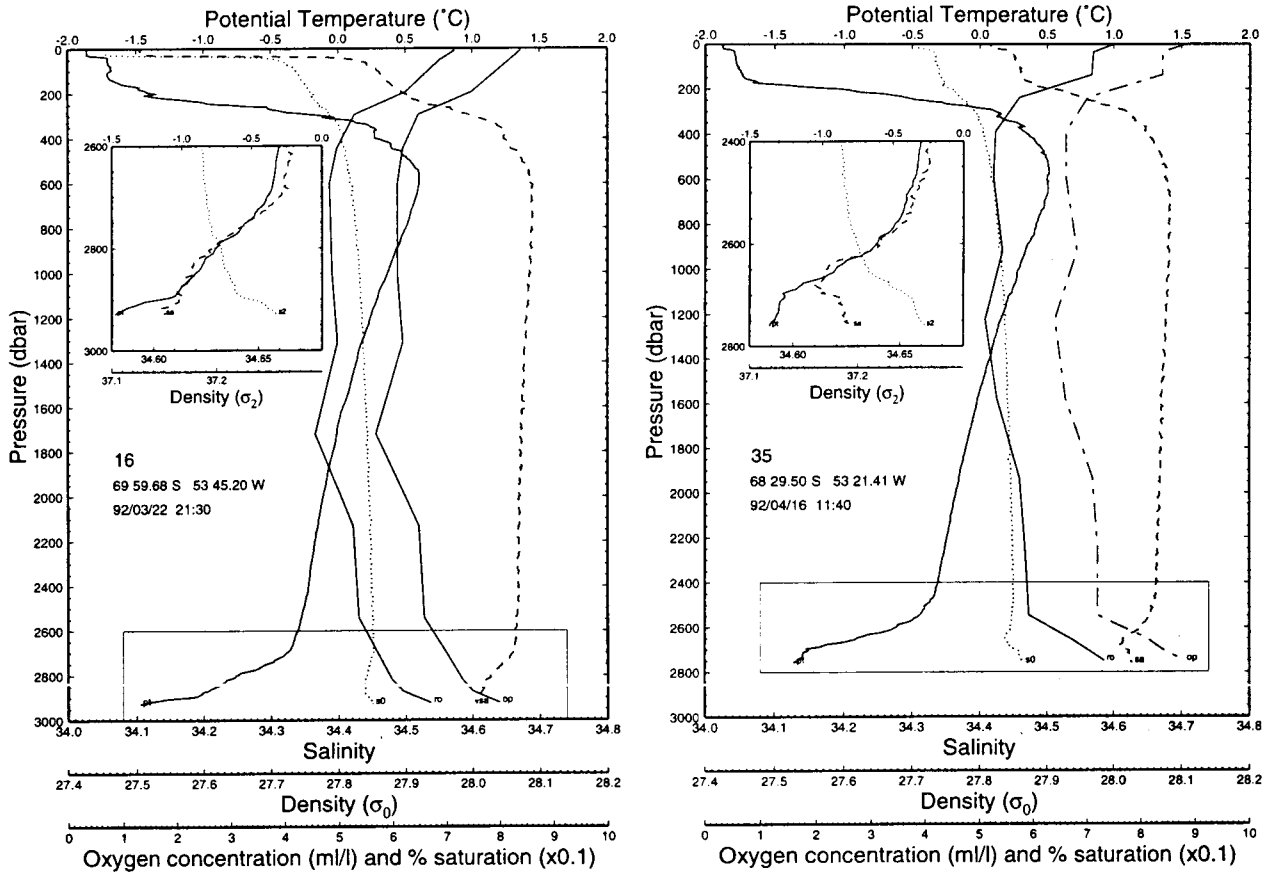

Fig. 3a and 3b. Profiles of potential temperature (PT), salinity (SA), sigma-0 (SO), rosette bottle oxygen (RO) and oxygen saturation (OS) vs. pressure (in dbar, roughly equal to meters) for typical Ice Station CTD casts. The insert shows the lower 400 dbar of the water column, using sigma-2 (S2, the density referenced to 2000 dbar).

drift. Remnants of the summer surface water were not fully removed until station 45 (May 1, 1992), and by station 35 the surface to 50 m salinity contrast is only a tenth of the difference measured at station 16, twenty-five days earlier.

Below the WDW, a thin, cold, oxygenated benthic layer is the most dramatic stratification of the western Weddell Sea. This feature has continuity with the benthic layer over the adjacent continental slope and is considered to be the seaward extension of plumes that drain the shelf of dense water. The very low temperature (<-0.8°C) of the benthic layer identifies it as WSBW [*Carmack*, 1974, 1982]. The sharp drop in temperature as the sea floor is approached begins near the -0.6°C isotherm. For ice camp stations 5 to 60 the thickness of the layer colder than -0.6°C is 127 m with a standard deviation of 33.6 m. From station 61 to 70, the ice floe drifted to shallower water, near 2500 m, and the benthic layer thickens rapidly, with a mean thickness of 289 m and a standard deviation of 172 m. *Gordon et al.* [1993] state that the temperature salinity relationship within this thicker benthic layer indicates vertical mixing, but with some added inflow of cold shelf water, as also noted by *Weppernig et al.* [1996] using Ice Station stable isotope data. The thin, stratified benthic layer persists in deeper water to the north and east of the northern limits of the ice station data (e.g. *Palmer* cruises 92-1 and 92-2 stations 4 and 2, both in just over 3000 m of water; and at *Palmer* 92-2 stations 7 and 8 in approximately 4300 m), indicating that benthic layer mixing is stronger over the inshore, steeper slopes of the northwest Weddell Sea.

Over the southern flank of the Scotia Ridge at *Palmer* 92-2 stations 10 and 11 (Figure 1) at 3700 m a

thick benthic layer has identical T/S properties to the thick layer at the northern ice camp stations. Similar mixing processes have either extended to this region or, more likely, the thick benthic layer produced to the west is advected and has descended to deeper water along the South Scotia Ridge. Additionally, a significant descent of the thin, more stratified WSBW benthic layer occurs further offshore in the northwestern Weddell Sea. The promontory of shallower topography east of Joinville Island narrows access to Powell Basin [*Tectonic Map of the Scotia Arc,* 1985] and may guide this flow into deeper water. WSBW that enters the Powell Basin endures a longer pathway and is exposed to greater amounts of vertical mixing.

The benthic layer at station 35 (Figure 3b) displays a salinity minimum (s-min) of 34.608 and a potential temperature of about -1°C, 100 m off the sea floor, with a much colder bottom salinity maximum (s-max) of 34.616. This salinity sequence within the cold benthic layer is observed at many of the ice floe stations and reveals the presence of two types of WSBW, with differing thermohaline histories, within a single water column [*Gordon et al.* 1993]. Station 16 (Figure 3a) shows only the s-min variety, indicating that the saline WSBW is injected into the deep ocean at a site further to the north. The upper portion of the benthic layer from the -0.5°C to the benthic s-min would be unstable in sigma-0, the density calculated at one atmosphere pressure, e.g. 27.850 at 2300 m and 27.844 at 2600 m on station 35. However, density referenced to higher pressures indicates *in situ* static stability, e.g., sigma-2 of 37.183 and 37.198 for the same depths. This reveals the important role of the thermobaric effect, i.e., that cold water is more compressible than warm water [*McDougall,* 1987] in stabilizing the deep water column and presumably in driving deep convection. Since the upper part of the benthic layer is stable only at pressures greater than 500-800 dbar, surface water contributing to the s-min must extend below 800 dbar before the thermobaric effect can produce free convection to the sea floor.

Oxygen concentration within the high salinity bottom water in contact with the sea floor nearly matches surface water levels. At station 35 oxygen concentrations are 7.48 ml l^{-1} at the sea surface and 7.33 ml l^{-1} at the sea floor. Both surface and benthic oxygen concentrations are about 85% of saturation. Within the s-min layer the oxygen concentration is about 80% of saturation, 6.67 ml l^{-1} at station 35 and 6.72 ml l^{-1} at station 16. For all Ice Station measurements, the bottom oxygen averages 6.73 ml l^{-1}, 80% of saturation with a standard deviation of 0.31 ml l^{-1}. Bottom oxygen is highest (over 7.0 ml l^{-1}) at stations 26, 35, 37, 38 and 39, which have a strong bottom salinity maximum (s-max) representation, although not all stations with strong bottom s-max have oxygen concentration >7.0 ml l^{-1}. These stations fall along the southern flank of a zonally oriented ridge near 68.4°S (Figure 1) which may guide seaward outflow of WSBW, perhaps within the Endurance Canyon [*Schenke et al.,* this volume]. The similarity between surface water and benthic layer oxygen concentrations indicates that surface water reaches the sea floor without much dilution by the oxygen poor WDW. Oxygen saturation decreases with distance from the sea floor, but a thin "inner" sheet of the descending plume is apparently protected by the outer layers of the plume from significant mixing with WDW.

Weppernig et al. [1996] find that the s-min water within the benthic layer is enriched in helium (^{4}He), a clear sign of glacial melt, which they deduce is drawn from Ice Shelf Water formed beneath the Filchner-Ronne Ice Shelf. The bottom s-max layer is lower in ^{4}He but is depleted in oxygen isotopes (δ^{18}O), also indicative of glacial melt. However, the s-max lacks the high ^{4}He signal, and is inferred to be that derived from Western Shelf Water (or High Salinity Shelf Water, HSSW) which contains glacial melt from the leading edge of the ice barrier, but has lost its ^{4}He to the atmosphere. *Weppernig et al.* [1996] indicate that the contribution of Filchner-Ronne Ice Shelf Water diminishes toward the north, but that slightly elevated ^{4}He concentrations at stations 38 and 44 suggest a possible meltwater contribution from the Larsen Ice Shelf (Figure 1), as also suggested by *Fahrbach et al.* [1995] and *Muench and Gordon* [1995]. Using CFC and tritium data collected during the Ice Station drift, *Mensch et al.* [this volume] find a nearly uniform influx of newly formed WSBW from the western edge of the Weddell Sea.

Weppernig et al. [1996] calculated that about 70% WDW, 25% shelf water and 5% surface water is required to produce the properties of the <0°C water. The average oxygen concentration at station 16 (Figure 3a) for water colder than 0°C is 5.5 ml l^{-1}, and WDW has an oxygen concentration of 4.86 ml l^{-1}. The shelf water would thus need an oxygen concentration of 7.3 ml l^{-1}, about what is observed adjacent to the Ronne Ice Shelf [*Gammelsrød et al.* 1994]. However, as noted above, the high bottom oxygen in the benthic layer implies that purer forms of shelf water descend to the deep sea floor. Within the benthic layer, bottom oxygen of approximately 6.8 ml/l, only 0.5 ml/l below that of the shelf water, blended with WDW oxygen of 4.8 ml/l imply a

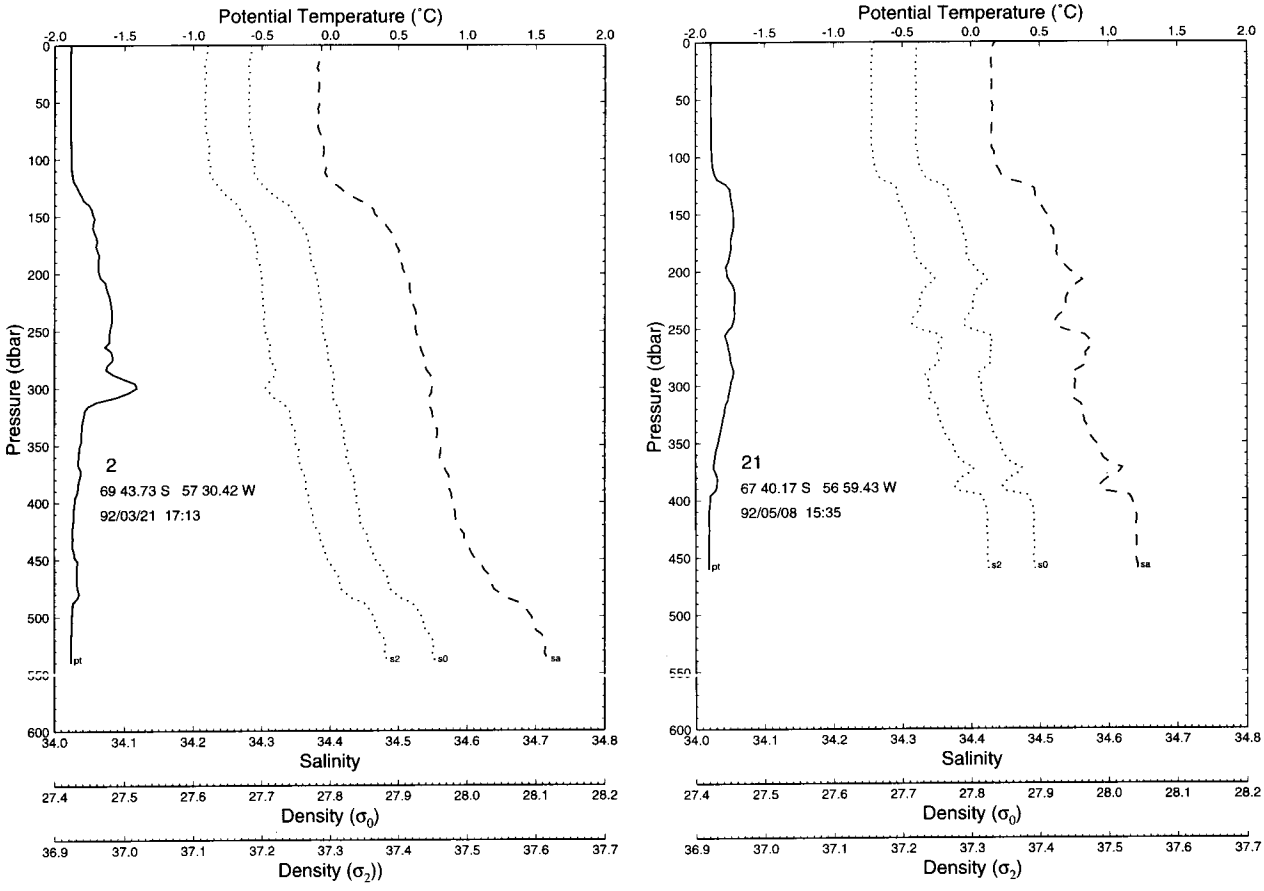

Fig. 3c and 3d. As in Figure 3a, but for typical continental margin stations obtained by helicopter. No oxygen data were obtained at the helicopter stations.

ratio of shelf to deep water of 80:20. The *Weppernig et al.* [1996] and *Mensch et al.* [this volume] studies combine tracer budgets and the *Foster and Carmack* [1976a] mixing recipe to infer that ≈5 Sv of bottom water colder than 0°C is formed in the Weddell Sea, similar to the value derived from geostrophic calculations by *Muench and Gordon* [1995] (Section 5).

4.1.2 *Continental Shelf*

Over the continental shelf, the profiles in Figures 3c and 3d reveal near freezing point surface and bottom temperatures (-1.88°C), with a weak maximum (t-max, -1.4°C at station 2; -1.71°C at station 21) at mid-depth, marking an intrusive remnant of WDW. Salinities range more widely from 34.39 at the surface to 34.72 at the bottom (540 m) of station 2. The continental shelf t-max core layer salinity of 34.55 is not the water column maximum, as is the situation within the deep water column. Station 21 salinity ranges from 34.43 at the surface to 34.64 at the shelf floor (460 m). The bottom potential temperature and salinity at station 2 matches that of the HSSW next to the Ronne Ice Shelf [*Gammelsrød et al.*, 1994], and is presumably advected from that region along the western shelf of the Weddell Sea (section 4.3).

4.1.3 *Potential temperature versus salinity for profile stations*

The θ/S range of water masses of the western edge of the Weddell Sea (Figure 4) shows that surface water covers the low salinity range near the freezing point of sea water. Toward higher salinity values, warmer water indicates the presence of WDW, more evident within the deep water, where it is separated from the surface water by a rather weak pycnocline. Dilute forms of WDW spread onto the continental shelf, forming the weak shelf t-max. With increasing depths from the WDW t-max core layer, salinity gradually decreases to the

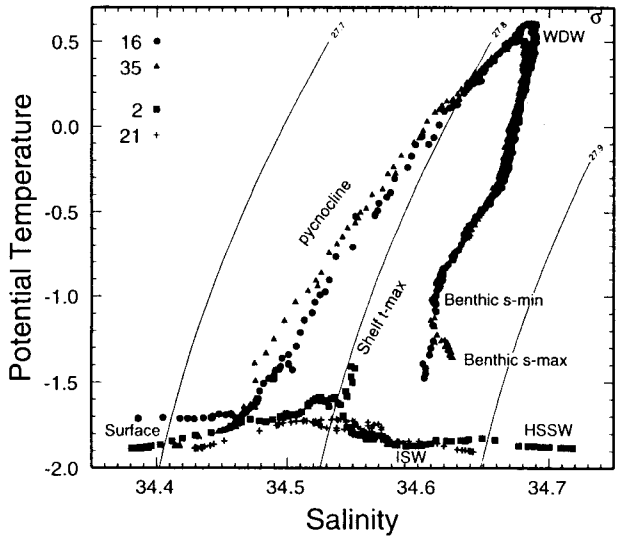

Fig. 4. Potential temperature (°C)/salinity (psu) diagram for the stations in Figure 3, with sigma-0 isopycnals. WDW is the Weddell Deep Water; HSSW is High Salinity Shelf Water; ISW is Ice Shelf Water. Shelf t-max is the shelf water temperature maximum. Also labeled are the pycnocline, surface water and benthic salinity minimum and maximum.

benthic s-min, which is often undercut by the more saline form of WSBW, forming a bottom s-max.

The densest water observed over the shelf represents northward spreading of HSSW from the southwestern shelf [*Gammelsrød et al.*, 1994]. The cold lower Ice Shelf Water is also widespread, with its low $\delta^{18}O$ and high ^4He values indicating that it contains glacial meltwater. It results from HSSW that has spread below the ice shelves, where it melts glacial ice, assisted by the pressure induced lowering of the sea water freezing point [*Schlosser et al.* 1990]. On the basis of the θ/S relationship, the Ice Shelf Water can be viewed as a source for the low salinity WSBW, and HSSW as the source for the high salinity WSBW.

4.2 *Sections*

Meridional Section. A meridional section (Figure 5) depicts the thermohaline stratification of the southern inflow and northern outflow of the western boundary current. The *Fedorov* stations from 47° to 52°W represent the southernmost crossing of the lower continental slope. Both temperature and salinity fields show the characteristic deepening of the interface between the cold, low salinity surface layer and the relatively warm, saline WDW as the continental margin is approached from the deep ocean. This marks the geostrophic adjustment of the stratification within the western boundary current. Here the core of the WDW t-max lies between 500 and 700 m, substantially deeper than the 200 to 300 m depths within the gyre interior [*Gordon and Huber*, 1990]. The t-max core exceeding 0.6°C at station 6 is part of a filament of more concentrated WDW carried within the axis of the western boundary current (Section 5.2). Seaward of the >0.6°C WDW axis, Ice Station CTD casts 7 and 8 and Fedorov stations 1 and 2 (Figure 1; *Huber et al.* [1994], reveal homogeneous temperature and salinity layers of up to 100 m in thickness from the lower pycnocline to the t-max. These are similar to steps attributed to double diffusion by *Muench et al.* [1990a] and *Muench* [1991]. Helicopter CTD stations (particularly station 4), *Palmer* 92-1 (station 2) and *Palmer* 92-2 (stations 6, 7 and 8), all east of the ice station trajectory, also display step stratification within the pycnocline. Double diffusion is more active east of the continental margin and seaward of the axis of the warmest t-max (section 5.2).

Bottom temperatures below -1.0°C indicate injection of cold WSBW east of the Fedorov stations. The Fedorov section shows this cold benthic layer is fresher than 34.61, clearly a product of the Ice Shelf Water variety of WSBW [*Foldvik et al.*, 1985b], though not necessarily drawn from as far east as the Filchner Depression (section 5.3). Within the central portion of Figure 5, the 500 - 700 m WDW t-max cools northward while the bottom temperature warms from -1.5°C to -1.2°C. The benthic layer is generally low in salinity, but a higher bottom salinity produces an s-min slightly offset from the sea floor. This bottom s-max is first observed at station 19 as a 0.01 salinity increase in the lower 20 m, and by station 26 this feature has mixed 50 m upward into the benthic boundary layer. The bottom s-max exceeds the overlying s-min by 0.01 on stations 19, 25 to 28, 35, 38, 47 to 49, and 61, showing no apparent correlation with bottom depth. A slight tendency at these stations for a thicker benthic layer (distance between the sea floor and the -0.6°C isotherm), indicates that the more regionally common s-min variety of WSBW is displaced upward by the salty variety.

The northern end of Figure 5 (the *Palmer* 92-2 section), extends to the southern flank of the South Orkney Island platform, crossing the cold outflows from the Weddell Sea. The shallowest expression of the WDW t-max marks the gyre axis at station 7 near 64.5°S. The WDW t-max along the section generally ranges between 0.4° and 0.5°C, exceeding 0.5°C only in

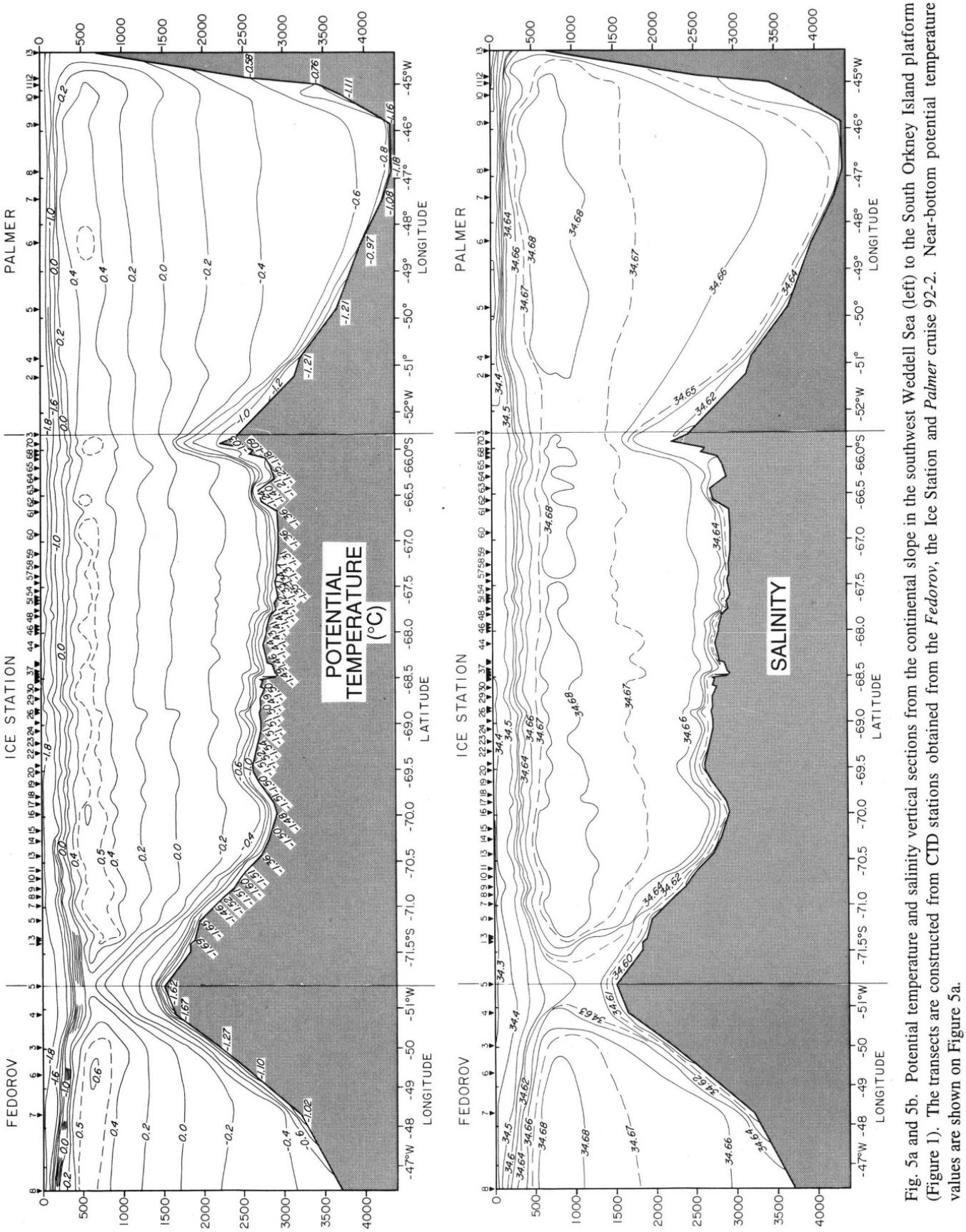

Fig. 5a and 5b. Potential temperature and salinity vertical sections from the continental slope in the southwest Weddell Sea (left) to the South Orkney Island platform (Figure 1). The transects are constructed from CTD stations obtained from the *Fedorov*, the Ice Station and *Palmer* cruise 92-2. Near-bottom potential temperature values are shown on Figure 5a.

a narrow feature at station 6 (Section 5.2). The WDW t-max core also attenuates as the South Orkney Islands are approached, marking the deep water expression of the Weddell-Scotia Confluence [*Foster and Middleton*, 1984; *Patterson and Sievers*, 1980; *Muench et al.*, 1990b; 1992] which advects continental margin water from the western Weddell Sea over the South Scotia Ridge. It is unlikely that active slope plume convection is present at the South Orkney Islands, as very cold and saline shelf waters are not present there. The eastward flowing cold bottom water is captured mainly by stations 7 to 9, with a bottom (4342 dbar) temperature of -1.17°C and salinity of 34.618 at station 8. This appears to mark advection into deeper water of low salinity WSBW derived from the southwest (section 5.3).

Shelf-Slope Sections. The four sections obtained from helicopter-deployed CTD casts, each supplemented by an ice camp station, provide cross-sections of the continental margin thermohaline structure (Figures 6, 7, 8, 9). Common features include; (a) Near freezing point water on the floor of the continental shelf spans a wide range of salinity beneath a weak temperature maximum marking modified WDW. (b) A thermohaline front (the Antarctic Slope Front) runs along the shelf-slope transition, and is comprised of a strong thermal front and a deep wedge of low salinity water referred to here as the pycnocline trough. (c) The pycnocline slopes to deeper depths eastward from the ice station trajectory and the shelf-slope front, a geostrophic expression of the western boundary current. (d) A sheet of very cold water, ≈100m thick, is draped over the continental slope and adjacent deep water, a product of convective plumes.

70°S Section. The southernmost helicopter section (Figure 6) crosses a deep outer shelf, with the shelf break occurring near 700 dbar. Water along the shelf floor is near the freezing point with a salinity greater than 34.7, matching that of HSSW found over the broad shelf adjacent to the Ronne Ice Shelf [*Gammelsrød et al.* 1994]. Given the lower horizontal resolution of this section, a low salinity pycnocline trough is suggested over the upper shelf slope region, the inshore component of which may be considered the Antarctic Slope Front [*Gill*, 1973; *Killworth*, 1977; *Jacobs*, 1991]. The deepest point of the pycnocline trough marks the convergence of sinking water from the shelf regime with offshore pycnocline water.

68°40'S Section. The shallowest outer shelf (about 300 m) was crossed on this section (Figure 7) and may be linked to a more extensive east-west ridge near 68°20'S that reaches into the deep ocean (Figure 1). The shelf floor salinity barely attains 34.6, as HSSW is blocked by the shallow outer shelf. The Antarctic Slope Front pycnocline trough is broad, with the deepest penetration (500 m) of the 34.6 isohaline at station 7 over the upper slope. The offshore pycnocline and particularly the WDW t-max deepen markedly as the slope is approached from the ice station trajectory. Modified WDW near -1.6°C is found over the shelf at 150 m, about 100 m shallower than that on Figure 6, but colder than the slope and bottom water, which approach -1.5°C. Stations 9, 8, 14 and 6 reveal a bottom salinity maximum at depths from 1400 to 2480 m, a feature lacking from ice station 24. This suggests that more than a single escape path is followed by salty shelf water enroute to the deep ocean. Unresolved local topography is likely to play a role governing exit sites, and the shallow shelf at 68°40'S is assumed to be a factor in driving HSSW to the deep ocean.

67°40'S Section. In sharp contrast to the section immediately to the south, the transect in Figure 8 crosses a narrow (10 km), well-defined slope front centered at station 28. The 34.6 trough-shaped isohaline reaches to nearly 600 m, and is continuous with the s-min core within the cold benthic layer. The sharpness and the deeper expression of this feature suggests a more focused convergence of shelf and slope water and an active convective process at the time of the observations. The low salinity trough follows the large horizontal temperature gradient. Over the 470 m outer continental shelf, salinity increases rapidly toward the shelf floor and is stratified as in Figure 6, although the shallower bottom depth prohibits the spreading of HSSW saltier than 34.7 from the Ronne Depression. Water colder than -1.7°C is in contact with the sea floor from the shelf break to station 29 at 1095 m, and displays a weak bottom s-max. A warmer bottom s-max is observed at 1280 m on station 18. Missing at station 25, the bottom s-max is re-established at 2235 m depth at station 19 with temperatures of -1.4°C. It forms the northward continuation of the bottom s-max seen at the 1990 to 2250 m depth range on stations 8 and 14 in Figure 7, 110 km to the south. This suggests only a minor (≈0.1°) downslope component at 2000 m, i.e. the slope plumes are nearly bottom isobath contour following currents. This descent angle is considerably less than the 5° reported by *Foldvik et al.* (1985a) at 700 m adjacent to the dense water outflow from the Filchner Depression. The Filchner outflow may be better guided by bottom topographic features, or more likely a greater

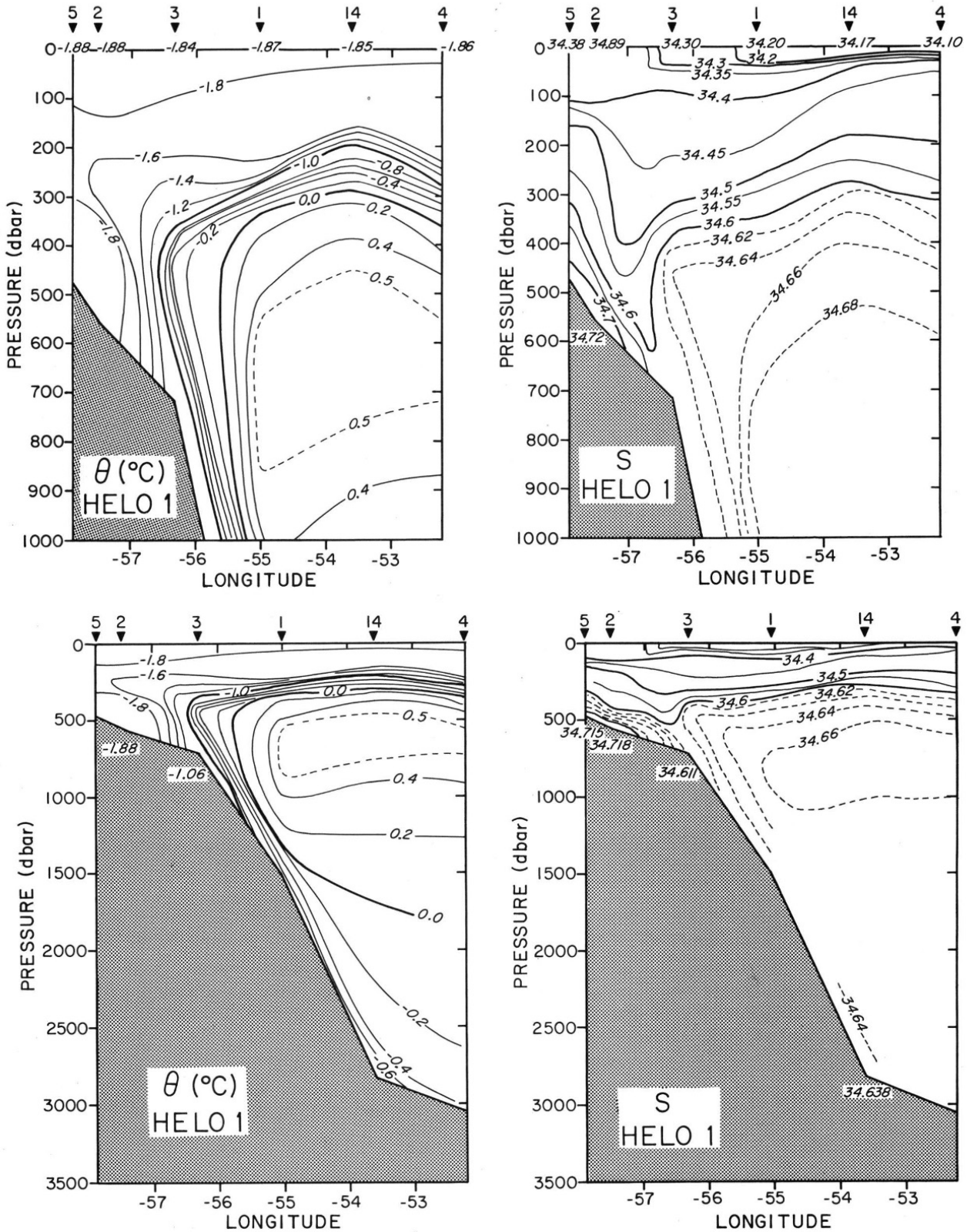

Fig. 6a-d. Potential temperature and salinity along helicopter section 1, 70°S (Figure 1), plus "14" from the Ice Station. The upper 1000 dbar is shown in 6a and 6b; the full water column in 6c and 6d, along with the near-bottom values.

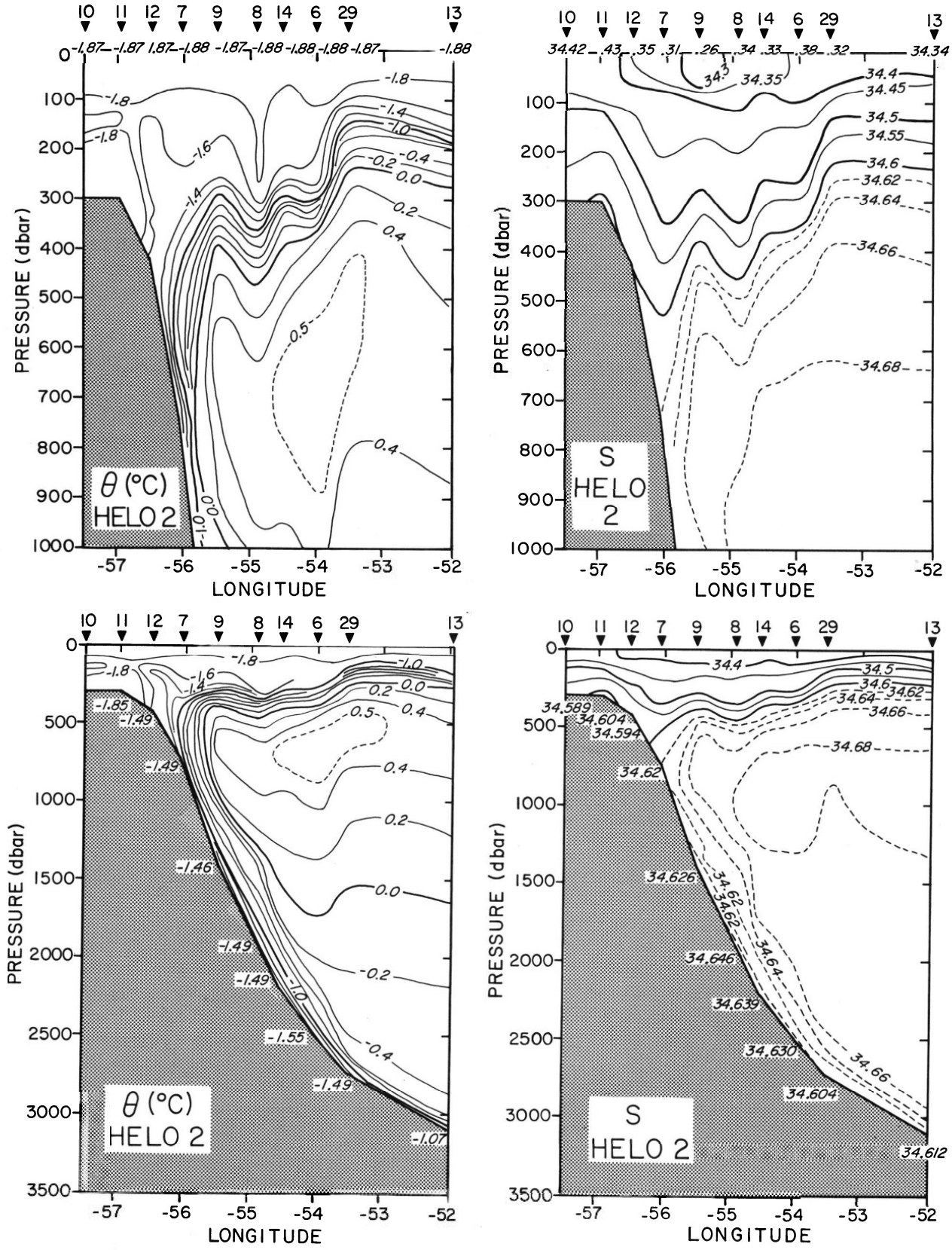

Fig. 7a-d. Potential temperature and salinity along helicopter section 2, 68°40'S (Figure 1), plus "29" from the Ice Station. The upper 1000 dbar is shown in 7a and 7b; the full water column in 7c and 7d, along with the near-bottom values.

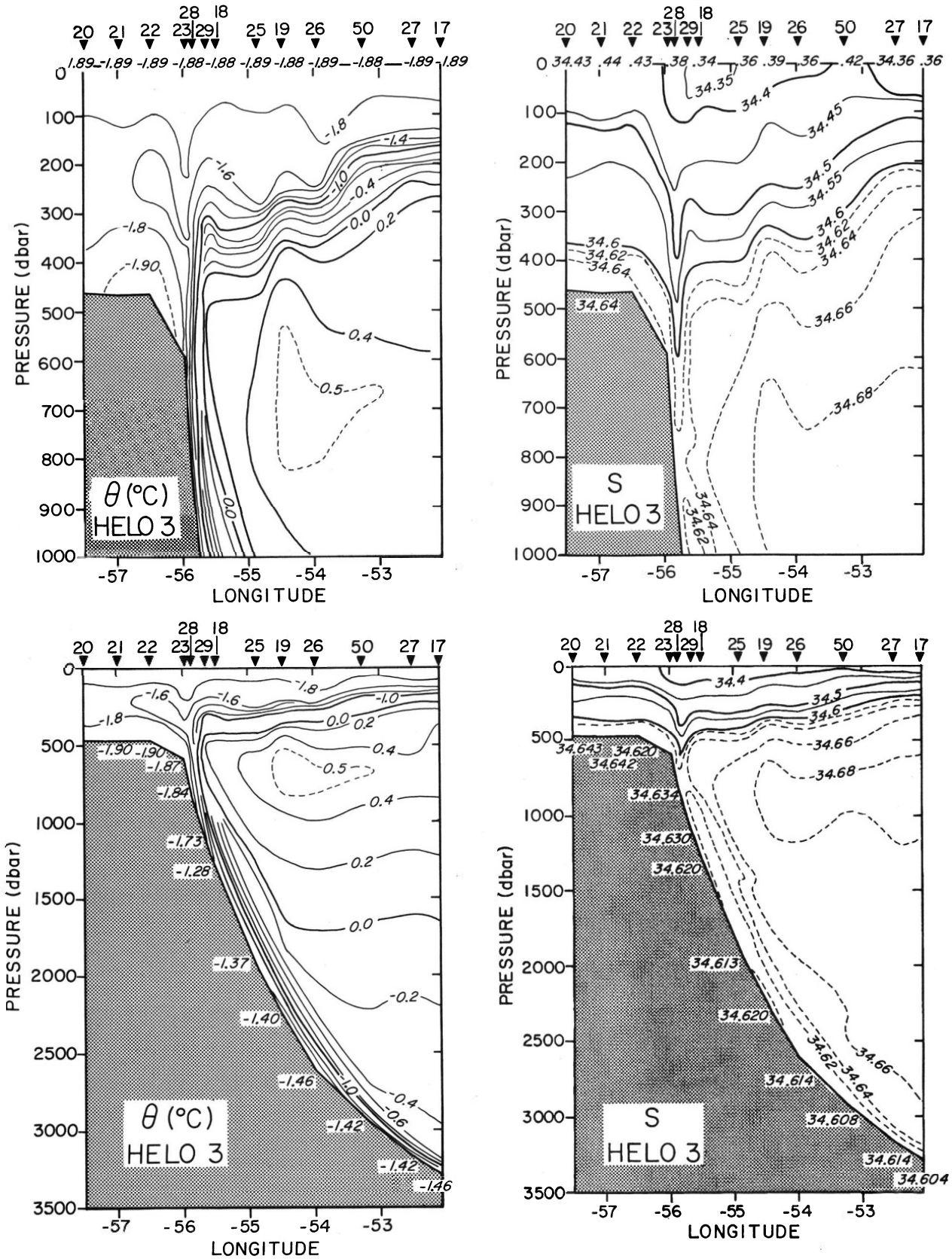

Fig. 8a-d. Potential temperature and salinity along helicopter section 3, 67°40'S (Figure 1), plus "50" from the Ice Station. The upper 1000 dbar is shown in 8a and 8b; the full water column in 8c and 8d, along with the near-bottom values.

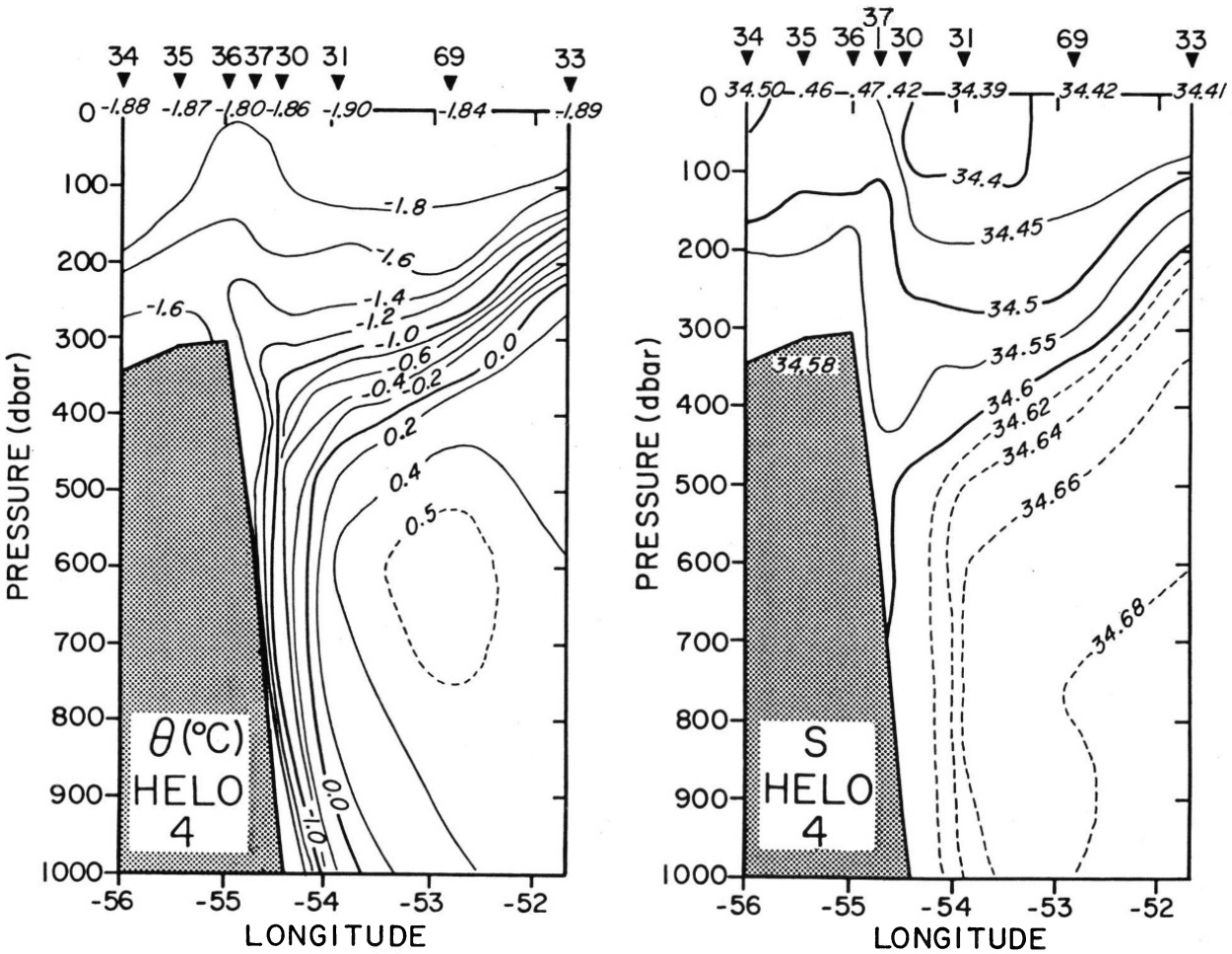

Fig. 9a and 9b. Potential temperature and salinity in the upper 1000 dbar along helicopter section 4, 65°50'S (Figure 1), plus "69" from the Ice Station.

descent angle can be achieved within the upper 1000 m where negative buoyancy forcing and shear induced turbulence may be larger and slope canyons may be better defined.

65°50'S Section. Figure 9 crosses a shallow outer shelf at station 36, with a bottom sloping down toward the coast and blanketed by low salinity water, revealing an absence of HSSW. The pycnocline trough hugs the continental slope, displaced from the sea floor by higher salinity water only at station 31 at a depth of 1465 m. A sharp benthic layer penetrates only to 1500 m, below which warming and thickening are believed to be the consequence of more intense bottom mixing [*Gordon et al.*, 1993]. If the weak bottom s-max at helicopter station 31 is a continuation of the bottom s-max at station 29 (Figure 8), the 220 km descent from 1095 m there to 1465 m at station 31 again indicates a trajectory vs. isobath angle of slightly less than 0.1 degree. If the streamline stems from station 28, the angle increases to 0.2, but in either case a contour following bottom current is indicated at depths of greater than 1000 m.

4.3 *Group Potential Temperature/Salinity Relationship*

The representative potential temperature/salinity (θ/S) relationships (Figure 4) provided an introduction to the θ/S structure of the western Weddell Sea. The full θ/S data set is presented in Figure 10 and key parts (**A** to **J**) of the θ/S scatter are discussed below.

Surface and Pycnocline Water. The near freezing, low salinity surface water (**B**) is confined to densities less than ≈27.7 in sigma-0. Within a salinity

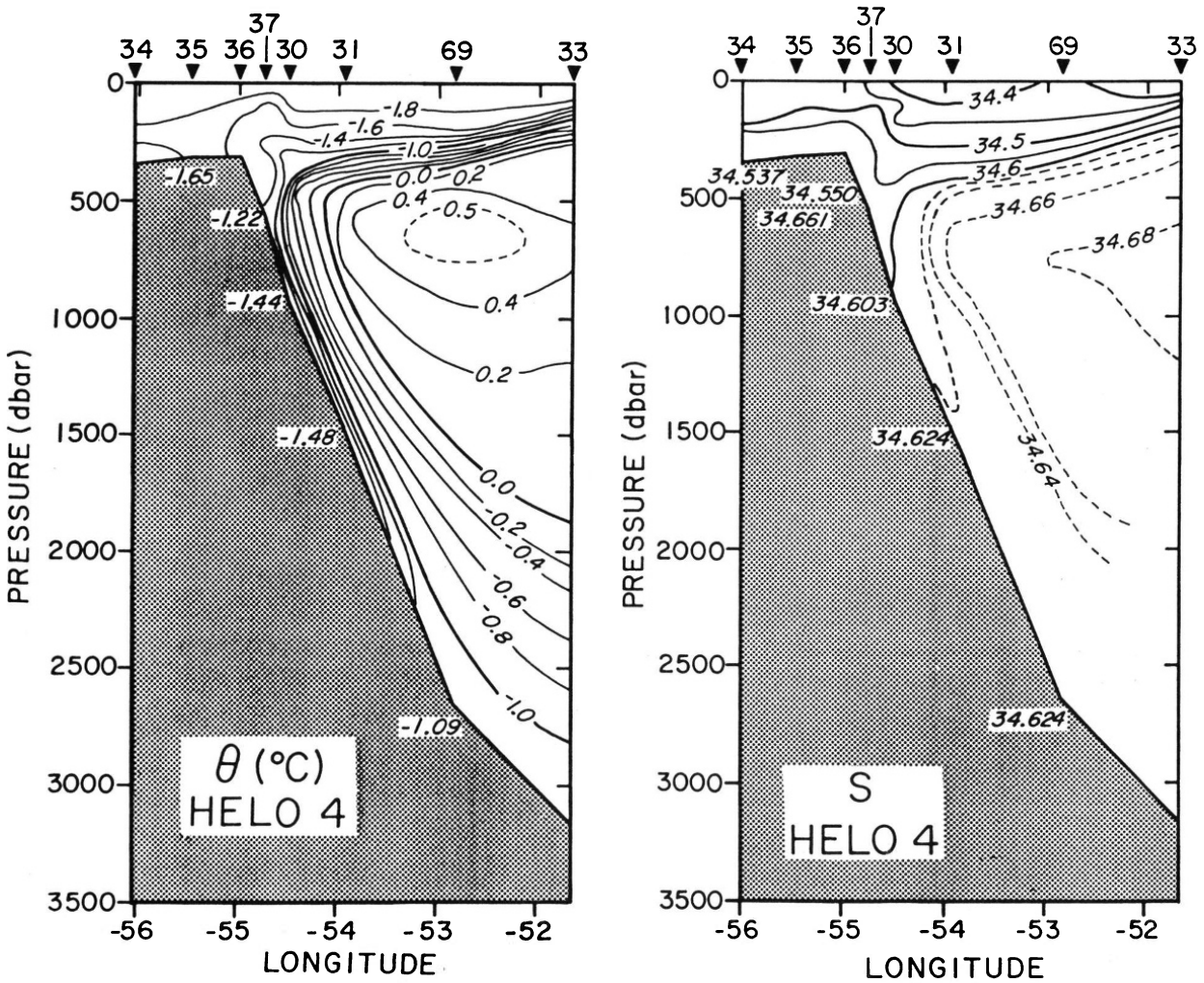

Fig. 9c and 9d. As in Figure 9a and 9b, but for the full water column, along with the near-bottom values.

range from 34.37 to 34.45 the surface layer gives way to warmer water marking the transition into the upper pycnocline. The salinity range within the upper pycnocline is large, amounting to 0.1 at the -1.5°C isotherm. Over the continental slope region the surface to pycnocline transition is gradual, occurring at relatively low salinity (**C**); further offshore a much more abrupt interface occurs at higher salinity (**D**) more characteristic of the interior Weddell Gyre. The low salinity upper pycnocline water may be related to greater stability and associated reduced vertical heat flux over the slope of the western Weddell Sea (section 5.1).

Weddell Deep Water. The θ/S relationship from the WDW t-max (at ≈0.5°C and 34.68 (**A**) to ≈-0.5°C and 34.65 (**A'**) is nearly a straight line. The linear θ/S relationship extrapolates to colder temperatures within the deeper water of the gyre interior, inhabited by the saltiest water in the -0.5° to -1.0°C interval, e.g. the *Palmer* 92-1 and 92-2 panels of Figure 10. Since straight lines in θ/S space denote two end-member mixing, this WDW lineage presumably represents a gyre scale blend of t-max water with the integrated (spatially and temporally mixed) AABW. The linear (**A** to **A'**) trend intersects the freezing point of sea water at 34.62, which can be provided by the high salinity WSBW, but not by the low salinity WSBW. The saline variety of WSBW may have been more dominant in the past than in the present [*Fahrbach et al.*, 1995; *Comiso and Gordon*, 1998]. An increase in the ratio of low to high salinity WSBW in recent decades may also result from accelerated production and escape of Ice

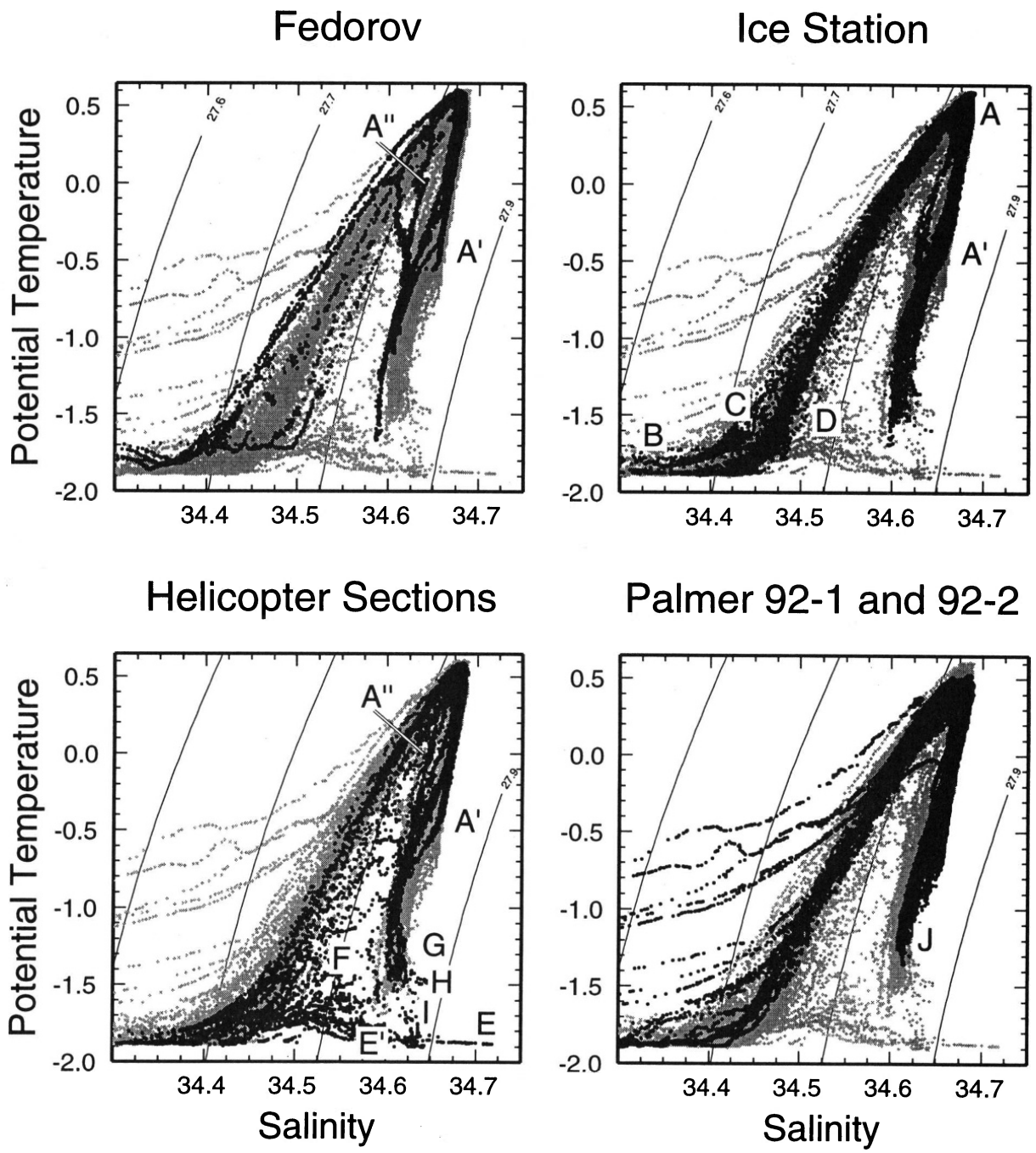

Fig. 10. Potential temperature/salinity diagrams for CTD stations taken from the *Fedorov* (upper left), the Ice Station (upper right), the helicopter (lower left), and the two *Palmer* cruises (lower right). The gray-toned dots are common to all panels and display all data; the black dots show the data from each source. The letters denote specific components of the water stratification: **A** is the Weddell Deep Water (WDW); **A'** the cold (≈ -0.5°C) end-member of the linear θ/S relationship below the WDW t-max; **A"** the continental slope θ/S segment from the t-max to -0.5°C, with lower salinity than within the Weddell Gyre interior; **B** the surface water; **C** the lower salinity upper pycnocline water; **D** the more saline upper pycnocline water over deeper water; **E** the High Salinity Shelf Water; **E'** the Ice Shelf Water; **F** is the continental shelf t-max; **G** the low salinity water within the benthic layer; **H** the high salinity water in the benthic layer; **I** the saline slope plume at the helicopter section along 67°40'°S; **J** the thicker, mixed benthic layer in the bottom water outflow south of the South Orkney Islands. The curved lines are lines of equal sigma-0.

Shelf Water, which may indicate increased glacial ice melt. Alternatively, more saline bottom water may have entered the Weddell sector in the past from the Australian-Antarctic Basin through Princess Elizabeth Trough near 82°E south of Kerguelen Plateau. *Speer and Forbes* [1994] and *Rintoul* [this volume] report bottom potential temperature of -0.45°C and salinity >34.673 within the Princess Elizabeth Trough, i.e., near the **A** to **A'** θ/S line, and state that this water flows westward. *Frew et al.* [1995] report westward flow in Princess Elizabeth Trough, and oxygen isotope data that suggest this water is not a product of the Weddell or Ross Seas, but is formed somewhere in the Australian-Antarctic Basin. However, it seems unlikely that transport of this water would be sufficient in relation to the WSBW production to play a dominant role in shaping the Weddell Gyre deep and bottom stratification.

At stations over the deeper southern portions of the continental slope, the θ/S relationship is bent toward lower salinities between the t-max and -0.5°C (**A'**). This low salinity WDW feature consistently falls to the shoreward side of the advective axis of the warmest WDW in the western Weddell Sea (Section 5.2), and to the seaward side of the slope front. The deviation from the linear θ/S trend occurs at warmer temperatures as the continental slope is approached. As access of shelf water to the t-max seaward of the slope front seems limited, it is proposed that the open ocean pycnocline of the western Weddell Gyre provides the source for this low salinity slope water. In effect, this would represent a direct open ocean modification of WDW adjacent to the continental slope. Such a process may account for attenuation of the deep water t-max as the continental slope is approached at nearly all longitudes around Antarctica. The cold end-member of the fan-shaped low salinity WDW feature (**A"** in Figure 10-*Federov*) occurs near -0.6°C and 34.62 at a sigma-0 of 27.840 (sigma-2 of 32.570). These density horizons mark the density limits of open gyre pycnocline access to the deep water.

Benthic Layer. Below -0.6°C the effects of the cold benthic layer are expressed in θ/S space as a gentle arc. Salinity decreases with temperature to an s-min (**G**) of ≈-1.1°C, below which the salinity either changes little or increases to a bottom s-max (**H**) around -1.5°C. The non-linear θ/S structure of the benthic layer indicates mixing between at least three end-members: warm WDW (**A**); the shelf floor s-max water (**E**) derived from HSSW at the freezing point and low salinity shelf water derived from Ice Shelf Water (**E'**), as corroborated by isotope data [*Weppernig et al.* 1996]. Helicopter stations 18, 23, 28 and 29 (Figure 8) provide strong evidence for a plume at <1300 m over the upper slope (**I**) linking in θ/S space dense shelf water with the cold benthic layer of the adjacent deep ocean. The θ/S relationship indicates that the freezing point shelf water responsible for this plume has a salinity of 34.64. Such water is observed along the 67°40'S and 70°S sections, but not along 68°40'S (Figures 6-8). The upper slope plume observed along 67°40'S may be derived from the local shelf region, consistent with the conclusion above that much of the slope plume descent occurs in the upper kilometer, perhaps channeled to the deep ocean by topography. Below a kilometer the plumes turn to follow isobath contours.

5. DISCUSSION

5.1 *Upper Layer and Perennial Sea Ice*

The Southern Ocean's sea ice displays a clear seasonal rhythm, with a February minimum extent of 3.4 to 4.3 million km^2 expanding to a September maximum of 18.0 to 20.2 million km^2 [*Gloersen et al.* 1992]. Winter and spring ocean and atmosphere studies within the seasonal sea ice cover indicate that oceanic heat and salt flux from the deep water to the winter mixed layer is a key factor in governing the ice thickness and rapid spring melting [*Gordon,* 1981; *Gordon and Huber,* 1990; *Martinson,* 1990; *Fahrbach et al.,* 1994a; *McPhee et al.* 1996]. The ice cover during the minimum period represents the perennial ice field, which is most extensive in the western Weddell Sea and in the Bellingshausen and Admundsen Seas. In the western Weddell Sea the perennial ice covers 1.2 million km^2. Within the perennial ice region, heat flux processes must be sufficiently different than in the seasonal ice zone to allow the ice to survive during the summer months. A key factor is the stability of the pycnocline, since a stronger pycnocline will act to attenuate vertical heat flux to the underside of the sea ice. The Bellingshausen and Admundsen Seas have low salinity surface water and a relatively warm t-max (Plates 10 and 46 of *Olbers et al.* [1992]), suggesting that deep water heat there is not vented to the surface layer. The Weddell Gyre has high surface salinity, a cold t-max and a weak pycnocline, all suggestive of strong deep to surface heat flux, as observed.

Robertson et al. [1995] found the average heat flux across the pycnocline beneath Ice Station Weddell to be only 3 W m^{-2}, in agreement with the microstructure study of *McPhee and Martinson* [1994] and the internal wave energy study of *Levine et al.* [1997]. The net flux within the western boundary current is less than the

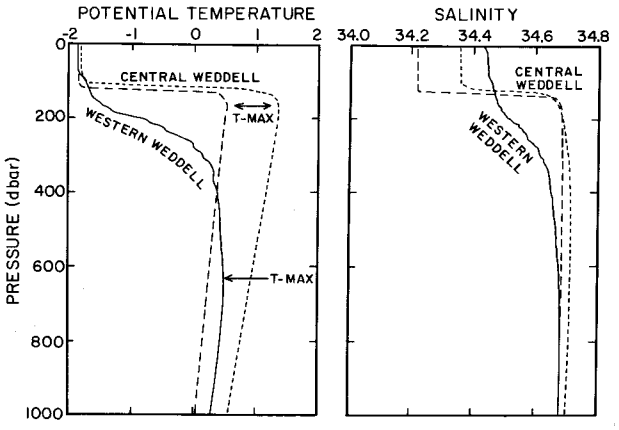

Fig. 11. Comparison between the potential temperature and salinity stratification in the western boundary current and that of the interior Weddell Gyre. The latter data are from 1986 measurements along the Greenwich Meridian [*Gordon and Huber*, 1990]. The western boundary current profiles are from Ice Station CTD 68 [*Huber et al.*, 1994].

Weddell Sea annual average of 19 W m^{-2} determined from a regional heat budget [*Fahrbach et al.*, 1994a]. This reduced heat flux and the colder atmosphere fed by prevailing winds from the south along the eastern flank of Antarctic Peninsula [*Schwerdtfeger*, 1975] conspire to produce the year round sea ice cover. Possible reasons, not mutually exclusive, for reduced vertical heat flux in the western and southern Weddell Sea include the relatively deep, inaccessible WDW heat source and the absence of mixing agents. The latter is suggested by the weak internal wave field [*Levine et al.*, 1997], and may be a positive feedback as the perennial ice could be expected to inhibit wind generated internal waves. In the western Weddell Sea, the depth of the deep water t-max is more than twice that within the interior of the Weddell Gyre, (600 m vs. 200 m in Figure 11), and is also slightly cooler, being further from the eastern WDW source (Section 5.2). Geostrophic balance within the accelerated western boundary current of the Weddell Gyre requires the deepening of isopycnals and corresponding WDW core layers. Consequently, the deep water heat is more remote from the sea surface processes and sea ice cover in the western sector, and mixing energy in the upper ocean may be insufficient to access this heat source.

An additional factor that may further inhibit vertical exchange processes is the presence of a relatively low salinity upper pycnocline over the continental slope (C in Figure 10; Figures 12a, 12b). A narrow band of lower salinity water centered on the -1.7°C isotherm within the upper pycnocline is located roughly over the 2000 m isobath. The low salinity band in Figure 12a occurs within a deeper segment of the -1.7°C isothermal surface (Figure 12b), slightly offshore of the pycnocline trough, which is aligned over the 800 m isobath (Figures 6-9). The source of this cold, low salinity feature may be the narrow shelf of the southeastern Weddell Sea (east of 25°W) where glacial meltwater mixes directly into WDW, suppressing AABW formation [*Fahrbach et al.*, 1994b]. Those authors estimate that 5.4 kg $m^{-1}s^{-1}$ (an upper limit) of glacial melt enters the coastal current in the eastern Weddell Sea. *Heywood et al.* [1997], also discuss the abundance of glacial meltwater entering the pycnocline of the eastern Weddell Sea. A section over the continental slope near 10°W in the eastern Weddell Sea [*Jacobs*, 1991] revealed a layer of water -1.8° to -1.5°C in temperature and 34.4 in salinity from 200 to 300 m over the upper slope. Presumably the Ekstrom Ice Shelf, about 20 km south of the southernmost station on that section, provides meltwater into this layer. The characteristics match those of the low salinity upper pycnocline of the Weddell Sea's western rim. As this feature falls within the helicopter sections, where technical difficulties prevented gathering of water samples for tracer determinations, we do not have stable oxygen isotope data that would help verify the glacial meltwater source of the western Weddell Sea's low salinity pycnocline feature.

5.2 *Weddell Deep Water*

The WDW t-max in the central segment of the Weddell Gyre (Figure 13a) is about 300 m below the sea surface, gradually deepening to 600-800 m over the continental slope. Water warmer than the 0.6°C t-max (Figure 13b) is found over a broad sweep of the central and southern segments of the Weddell Gyre. Warm WDW migrates westward from its origin in the warm circumpolar deep water along the eastern edge of the Gyre near 30°E. Cooling enroute is accomplished by entrainment into and mixing with winter surface waters and by lateral mixing with shelf water masses. The coolest WDW occurs in the western segment of the Gyre, the region most remote from the heat source. An important exception along the western boundary is a narrow band of >0.5°C t-max water, seaward of the pycnocline trough over the continental slope which marks the advective effects of the western boundary current. This current rapidly moves warm WDW water to the north and east, isolating a patch of older, cooler (<0.4°C) t-max water roughly between 40°-50°W and

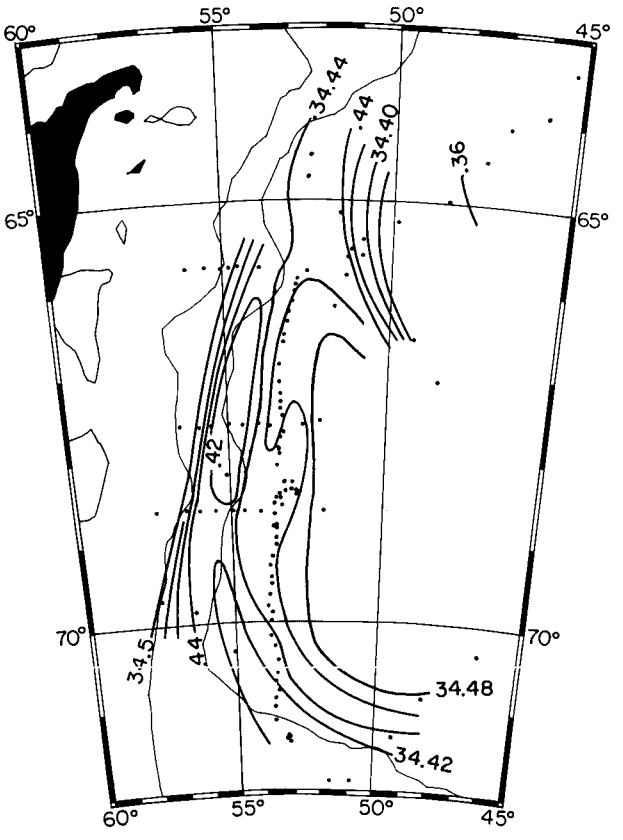

Fig. 12a. Salinity on the -1.7°C isotherm, based on the Ice Station Weddell data set. The "34" is omitted on some isohalines.

66°-71°S. It is proposed that pycnocline water produced within this isolated pool spreads along isopycnals into deeper water over the continental slope, from where it becomes incorporated into convective processes of the margins, forming the low salinity deep water feature **A"** in Figure 10. Shoreward of the warm advective core, the t-max cools rapidly, at first deepening within the pycnocline trough and then shoaling over the upper slope and onto the shelf as the modified WDW.A band of >-1.2°C t-max water occurs near 45°W over the western flank of the less than 500 m ridge (Berkner Shelf, *Gammelsrød et al.*, [1994]) and a secondary t-max intrusion is observed near 30°W.

5.3 *Weddell Sea Bottom Water*

As we collect more data, it becomes increasingly evident that the ocean varies in space and time far more energetically than previously thought. *Foster and Middleton* [1979] used 1975 and 1976 data across the outflow of bottom water from the Weddell Sea to show temporal variability in bottom stratification. *Fahrbach et al.* [1995] found that bottom water transport in the western Weddell Sea varied from 0.7 Sv to 3.9 Sv from late 1989 to late 1992, with a suggestion of a seasonal cycle in which minimum bottom temperature and maximum velocity occurred in early austral summer. *Comiso and Gordon* [1998] reported that the bottom water of the western Weddell Sea in the early 1990's was colder and fresher than observed in previous decades, which suggests relative weakening of the saline variety of bottom water. Detailed maps of bottom potential temperature and salinity (Figures 14a and 14b) also reveal a more complex pattern of multiple streams of differing types of bottom water.

The warmest bottom water of the region, >-0.4°C in Figure 14a, is advected into the Weddell Sea from the east over the continental slope. The core of this water is near 1000 m, well below the 600-650 m depth of the mouth of the Filchner Depression or Trough [*Schenke et al.*, this volume]. The warm bottom water is lifted

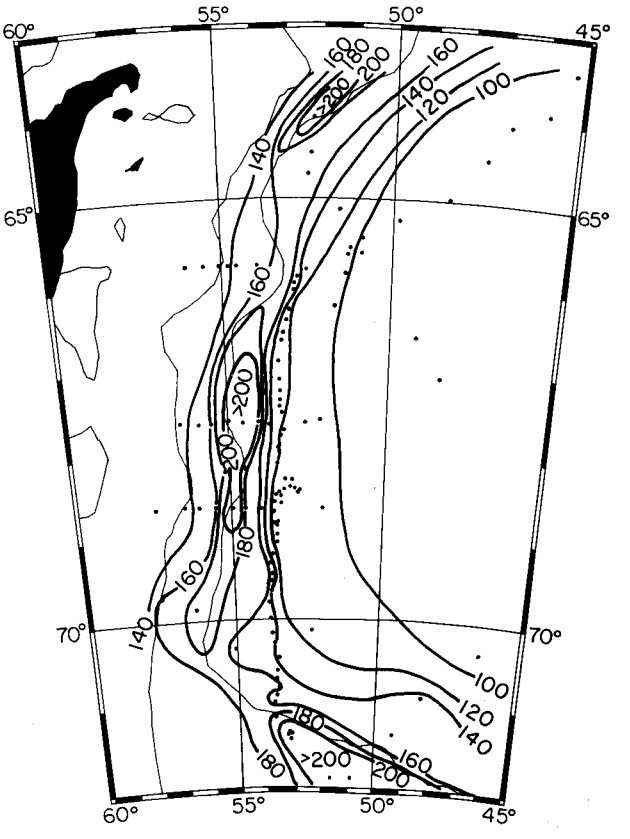

Fig. 12b. Pressure (dbar) of the -1.7°C isotherm based on the Ice Station Weddell data set.

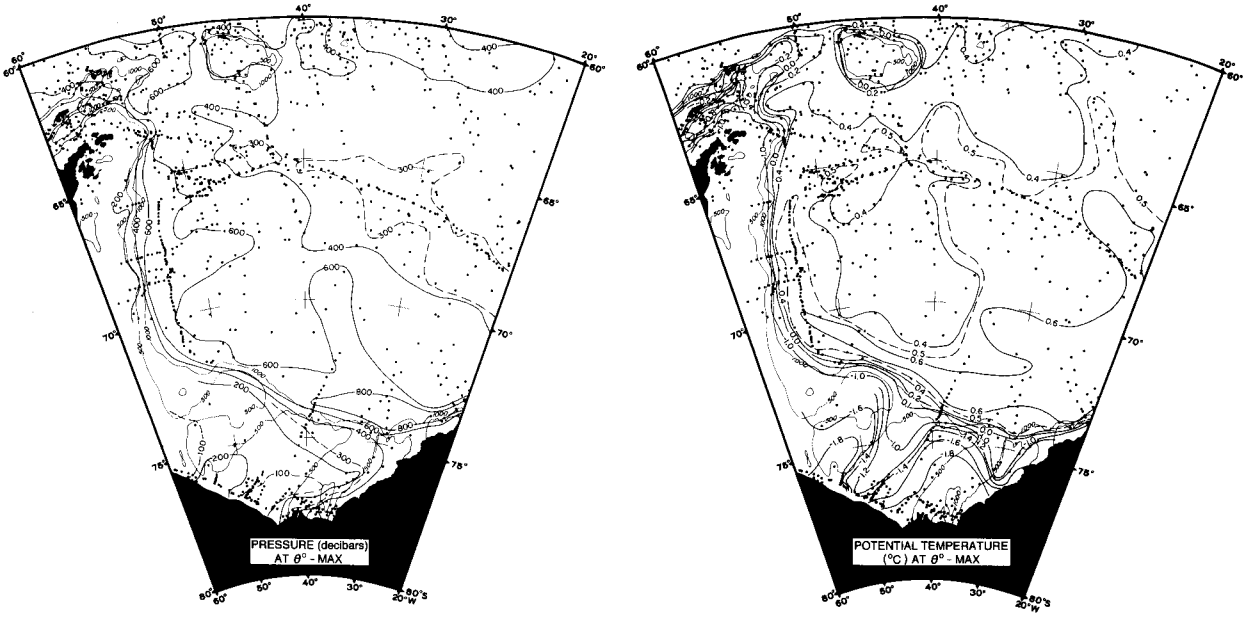

Fig. 13a and 13b. Pressure and potential temperature at the western Weddell Deep Water potential temperature maximum (θ-max) core layer, constructed from archived Weddell Sea data. GB and FD show the locations of the General Belgrano Bank and Filchner Depression. The 500 to 1000 m isobaths are also shown.

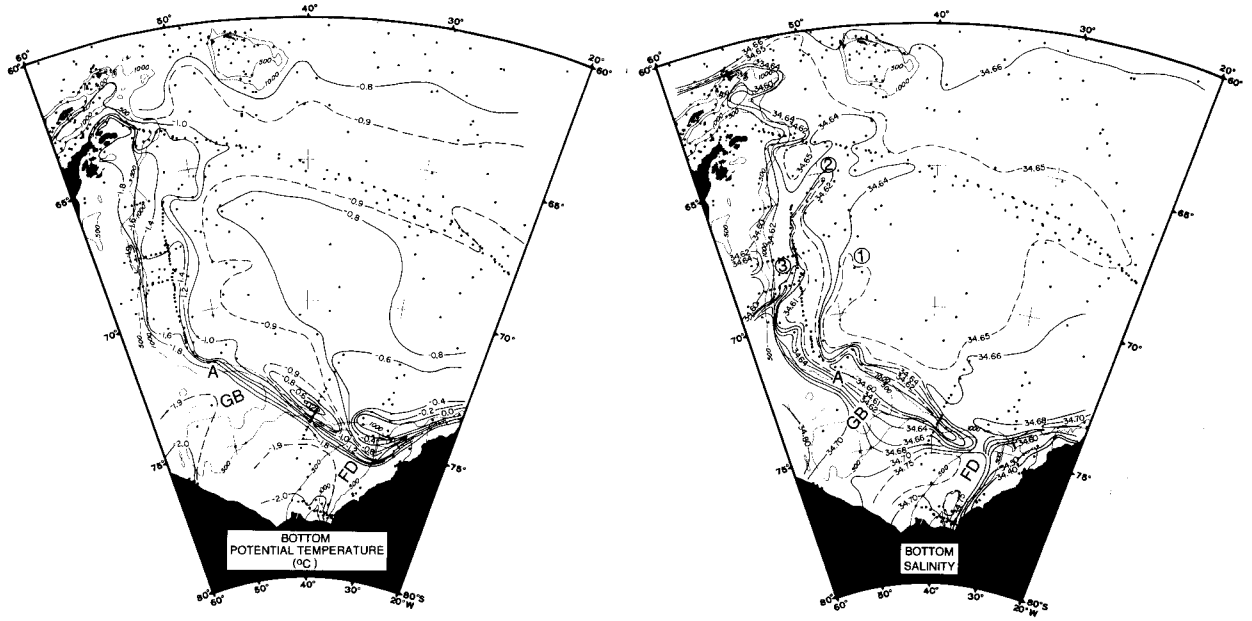

Fig. 14a and 14b. Potential temperature and salinity of the Weddell Sea Bottom Water (WSBW) based on observations within 50 m of the sea floor. The circled numbers 1-3 represent the primary plumes of WSBW. Point A denotes the site of cold shelf water export into the deep ocean, leading to plume 2. Plumes 1 and 3 are drawn from the Filchner Depression and High Salinity Shelf Water, respectively. The 500 and 1000 m isobaths are shown.

off the sea floor by the dense, cold Filchner Depression outflow [*Foldvik et al.*, 1985a,b]. West of the mouth of the Filchner Depression the warmer bottom water reappears in contact with the continental slope sea floor, as the cold water plume drops to the deeper ocean. Within the deep central Weddell Sea a broad spread of relatively warm bottom water, -0.8°C, suggests an admixture of resident bottom water with Filchner Depression outflow.

While there is a scarcity of near-bottom data along the continental margin from 40° to 50°W, clearly the warm bottom water at 40°W is no longer in contact with the sea floor by 50°W. Because the warm bottom water has again been lifted off the sea floor, it is proposed that a major export of cold shelf water occurs near point **A** [Figure 14] just west of General Belgrano Bank (72.5 to 73.5°S and 47° to 50°W; **GB** on Figure 14), though with the available data export at the eastern flank of the General Belgrano Bank is feasible. The water colder than -2.0°C in the Ronne Depression west of General Belgrano Bank suggests the export of Ice Shelf Water generated at the Ronne Ice Shelf [*Gammelsrød et al.* 1994]. The ice station data clearly reveal the widespread presence of bottom water at temperatures well below -1.0°C over the continental margin west of General Belgrano Bank. From the bottom temperature pattern, and from the bottom salinity discussed below, it is improbable that the very cold bottom water of the western rim of the Weddell Sea is derived from the Filchner Depression outflow due to the lack of continuity of <-1.0°C water across the well-resolved 35°-40°W continental margin section.

North of point **A** the areal extent of the sea floor deeper than 1000 m and covered with bottom water colder than -1.0°C grows progressively larger south of 67°S. Most of the Ice Station bottom temperatures are well below -1.2°C in the western Weddell Sea at depths of 2500 to 3000 m. North of 67°S the width of the <-1.4°C bottom layer abruptly narrows, which may be due to increased vertical mixing with slightly warmer overlying water [*Gordon et al.*, 1993]. In the northwestern Weddell Sea cold bottom water (<-1.0°C) turns eastward and deepens near 64°S, continuing as a band of <-0.9°C water between 64° and 66°S as part of the northern limb of the Weddell Gyre.

The bottom salinity distribution (Figure 14b) provides further insight into the bottom water source and spreading patterns. An elongated plume of <34.62 bottom water (**2** on Figure 14b) follows a 700 km path from point **A**, its presumed source, to the vicinity of 65°S, 50°W. This area marks a further descent of low salinity WSBW water from 3000 db to greater than 4000 db, and feeds the cold 64°-66° band of bottom water along the northern limb of the Weddell Gyre. Bottom topography plays a role in guiding the bottom water to greater depths. East of point **A**, a low salinity bottom water feature implies that plume **2** could be derived from sinking of water along the northern boundary of General Belgrano Bank, rather than from the Ronne Depression. However, the low salinity (34.60) bottom data near 40°W and the 500 m isobath are above -0.8°C, too warm to be the source of the <34.62 low salinity plume (plume 2). As the -1.0°C isotherm is first seen in bottom water deeper than 1000 m at point **A**, the assumption of a Ronne Ice Shelf source is reasonable, although not proved. The *Weppernig et al.* [1996] study did not have a data distribution adequate to distinguish between a Filchner Depression or a Ronne Depression Ice Shelf Water source. *Gammelsrød et al.* [1994] find that the Filchner and Ronne Ice Shelves produce essentially identical Ice Shelf Water. A high resolution barotropic tidal model of the Weddell Sea [*Robertson et al.* this volume] reveals vigorous tidal currents over and slightly to the west of General Belgrano Bank and along the Ronne Ice Shelf front. Tidal induced mixing may play a critical role in the blending of ingredients that form WSBW [*Foster et al.* 1987], and provide a mechanism enabling cabbeling and thermobaric effects to become effective.

The HSSW of the western Weddell Sea [*Gammelsrød et al.* 1994], migrates northward along the continental shelf, escaping from the shelf as a saline plume (**3** on Figure 14b) just shoreward of the <34.62 plume. A slope canyon near 70°S may direct the saline shelf water into the deep ocean. The saltier (denser) bottom water lifts the lower salinity bottom water off the sea floor, inducing the s-min and s-max stratification within slope plume, as discussed above. The 1992 Ice Station data provide the first Weddell Sea observations of a saline bottom water variety, usually associated only with the Ross Sea. Seaward of the elongated <34.62 plume 2, a weak plume (**1** in Figure 14b) of >34.65 water has potential temperatures between -0.9° and -1.0°C. It is proposed that this feature is a mixture of the Filchner Depression outflow with the more saline bottom water advected into the Weddell Sea from the east.

In summary: three plumes of newly formed bottom water are injected into the deep Weddell Sea (**1, 2** and **3** on Figure 14b). The warmer, saline plume (**1**) represents a mixture of Filchner Depression outflow with warmer, more saline bottom water from the interior Weddell Gyre. The cold, low salinity plume (**2**) is derived from outflow of Ronne Ice Shelf Water exiting the shelf just west of General Belgrano Bank (point **A** on

Figure 14). This plume may be protected from mixing with the warmer, more saline interior bottom water by the Filchner Depression outflow, allowing its northward extension in concentrated form. The third plume is the cold, high salinity bottom water (**3**) formed from high salinity shelf water descending into the deep sea near 70°S and probably at other sites along the western rim of the Weddell Sea. Sustained variations in the relative strengths of these three plumes would induce changes in the bottom water of the Weddell Sea and beyond.

5.4 *Larger Scale Considerations of AABW Formation*

Using 1973 Weddell Sea geochemical data, the *Foster and Carmack* [1976a] WSBW mixing recipe and an estimate for basal melting of the Filchner and Ronne Ice Shelves of 2 x 10^{11} m^3 yr^{-1}, (accounting for the low deuterium and oxygen-18 isotope values), *Weiss et al.* [1979] determined a 5 Sv formation rate of WSBW. Using tritium data they determined a WSBW formation rate of 2.9 Sv. Most recent estimates fall in this range. *Muench and Gordon* [1995] estimated the total northward transport of 5 to 6 Sv within the lower 300-500 m of water colder than -0.4°C, (average -0.8°C) along the western rim of the Weddell Sea in 1992. For the period September 1989 to January 1993, *Fahrbach et al.* [1994a] found 2.6 Sv of WSBW, defined as water colder than -0.7°C, and 1.2 Sv of Weddell Sea Deep Water defined as having potential temperatures of 0°C to -0.7°C. *Fahrbach et al.* [1995] showed that WSBW transport averaged 1.7 Sv in 1991, the period with the most complete monitoring array, with a May maximum of 2.4 Sv and a January minimum of 0.8 Sv. They reported a high of 3.9 Sv in July 1992 and an average of ≈2.8 Sv during the time of the Ice Station Weddell drift. *Gordon et al.* [1993] estimated 3 Sv of newly formed WSBW (-0.8°C) in the western Weddell Sea.

The *Muench and Gordon* [1995] transport included water as warm as -0.4°, incorporating some of the deep water defined by *Fahrbach et al.* [1994a]. If the water between potential temperature -0.4°C and -0.7°C represents about half of the deep water transport (between the 0.0°C and -0.7°C isotherms), the *Muench and Gordon* [1995] transport estimate should be reduced to 4.0-4.8 Sv for the WSBW component above. As many assumptions are used in the various WSBW transport determinations, the difference between 2.8 Sv and 4.8 Sv may not be very significant. A working value for WSBW colder than -0.7°C (average of -1.1°C) may be taken as 3-4 Sv. This water is derived from the continental margin extending from the Filchner Depression and, in more dilute form, northward at least to the western station on helo section 3 at 67°40'S.

The global influence of this flux may be estimated from a thermal balance of the abyssal ocean (>4°C), the average temperature of which is about 1.7°C [*Gordon*, 1975, 1991]. The average temperature of WSBW within the benthic boundary layer is about -1.1°C, nearly 2.8°C below that of the abyssal ocean. As the WSBW is produced from converted abyssal water upwelling within the Weddell Gyre, the process of WSBW formation acts to remove heat from the abyssal ocean. The major provider of heat into the abyssal ocean is North Atlantic Deep Water (NADW, including a Mediterranean Sea source) which forms at a rate of about 15 Sv with an average temperature of about 2.7°C [*Gordon*, 1975] about 1.0°C above the average abyssal ocean temperature. A WSBW flux of 3.5 Sv at -1.1°C removes 4.1 x 10^{13} Watts while NADW adds about 6.3 x 10^{13} Watts to the abyssal ocean. Thus WSBW formation offsets about 65% of the NADW heating. Using the *Muench and Gordon* [1995] values for water colder than -0.7°C, WSBW removes 5.1 x 10^{13} Watts, offsetting 82% of NADW heating.

Colder bottom waters form in the Ross Sea [*Jacobs et al*, 1985; *Locarnini*, 1994], along the Adelie Coast [*Gordon and Tchernia*, 1972; *Rintoul*, this volume] in Prydz *Bay [Nunes-Vas and Lennon*, 1996], and probably other regions around Antarctica. Sinking of cold surface water that does not reach the sea floor is likely to occur over the slope and open ocean [e.g. *Carmack and Killworth*, 1978]. Convective cooling of the deep water to nearly 3000 m occurred during the Weddell Polynya period [*Gordon*, 1982]. Additionally, the Ice Station Weddell data suggest that pycnocline water from the interior of the Weddell Gyre may very well migrate toward the continental margin, sinking into the deep water on the seaward side of the Antarctic Slope Front. This may be quite common around Antarctica, as the water column over the Antarctic continental slope is significantly colder, lower in salinity and enriched in oxygen than is the water further offshore. Assuming all non-Weddell formation of waters colder than -1.7°C (WSBW equivalent) equals the Weddell production, then the total heat removal from the deep ocean by such processes in the Southern Hemisphere would be 8.2 x 10^{13} Watts. The Southern Ocean cooling may therefore not only compensate NADW heating, but help to balance an even larger source of heat to the abyssal ocean, i.e., downward diffusion of heat through the thermocline.

6. CONCLUSIONS

1) Two varieties of cold shelf water contribute to the formation of WSBW with a surprisingly small degree of dilution during sinking into the thin benthic layer. The denser HSSW, a product of sea ice formation, is drawn from the western Weddell Sea. The lighter ISW, a mixture of HSSW and glacial meltwater from the Filchner and Ronne Ice Shelves, is drawn from the Filchner Depression and western flank of General Belgrano (GB) Bank. Most of the Filchner Depression water mixes with warmer, saltier, resident AABW from the east to flood the deep central Weddell Sea. The persistent GB water, often layered above the saltier variety of WSBW, descends to >4000 m depths near 65°S, 50°W, feeding the cold bottom water band beneath the northern limb of the Weddell Gyre.

2) Indications from θ/S analyses that bottom water formed in recent decades is less saline than previously could imply an increase in the production and escape from the shelf of ISW, or a decrease in the inflow of bottom water from east of the Weddell Sea. The latter is considered unlikely to exert a strong influence on WSBW characteristics.

3) Cold, low salinity, high oxygen surface water sinks with little dilution by WDW, faster in the upper kilometer and more contour-following at greater depths. Geostrophic adjustment of the pycnocline in the boundary current, cabbelling and Ekman veering in the bottom boundary layer may trigger important thermobaric effects.

4) The characteristic deep low-salinity "V" or pycnocline trough of the Antarctic Slope Front (Figure 15) is defined on its north and east by Weddell Gyre pycnocline water, on its south and west by a variety of shelf waters, and in its upper core by meltwater from the southeast Weddell Sea. The lower salinity in the pycnocline trough accounts for its depth, as the static stability increases the pressure required to initiate thermobaric-induced convection. Low salinity near the slope front may also inhibit vertical heat flux, contributing to the perennial ice cover.

5) It is remarkable that the global influence of AABW stems from small scale processes at the Antarctic Continental Margin. In the southern and western Weddell Sea alone, the convergence of surface and pycnocline water at the slope front ventilates the entire water column, is advected into the ACC, and eventually compensates for 65 to 82% of the abyssal ocean heating by NADW formation. Deep ventilation will also occur when similar source waters and deep mixing processes occur at the slope front elsewhere around Antarctica. Given the scales and variability involved, it may be difficult for global circulation models to properly simulate AABW formation.

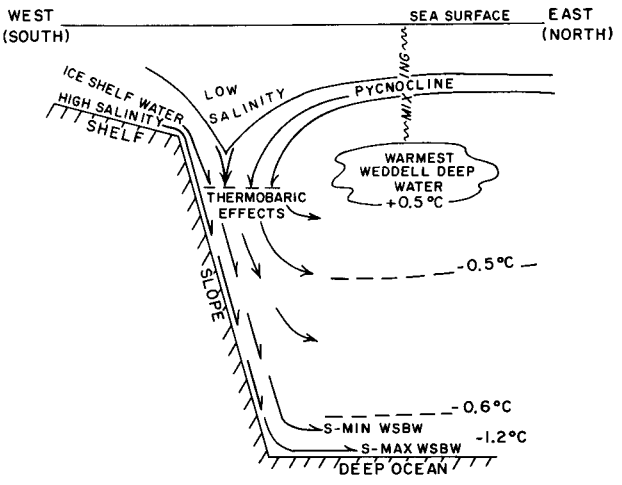

Fig. 15. Schematic illustration of the convective pattern of the western Weddell Sea, based on analyses of the Ice Station Weddell data set. Surface, shelf and pycnocline waters from a variety of deep ocean and continental shelf sources converge and sink within and adjacent to the main pycnocline trough associated with the Antarctic Slope Front.

Acknowledgments. I thank all those who contributed to the success of Ice Station Weddell, which was occupied under the most adverse conditions. Special thanks are due to P. Wilkniss, former director of the Office of Polar Programs, and to B. Lettau and A. Sutherland of NSF for their support of this risky venture. N. Kornilov from the Arctic and Antarctic Research Institute in St. Petersburg arranged for the very significant Russian contribution during a very difficult time. J. Evans of Antarctic Support Associates had the difficult task of procuring and shipping all of the material required for life and science support systems. The skills of Ice Station Manager V. Lukin of the Arctic and Antarctic Research Institute and J. Ardai of Lamont-Doherty Earth Observatory were the main reason for the success of the field operations. H. Hellmer, B. Huber, P. Mele, A. Ffield, T. Baker and D. Martinson from Lamont-Doherty Earth Observatory, L. Padman from Oregon State University and S. Ackley from the Cold Regions Research and Engineering Laboratory deserve special praise for collection of the valuable data sets from the ice station, helicopters and research ships. The comments of reviewers and editors were helpful in improving the presentation of this research. The Ice Station Weddell research was supported by a grant from NSF (OPP-93-13700) and a grant/cooperative agreement from NOAA (UCSIO P.O. 10058161). The views expressed

herein are those of the author and do not necessarily reflect the views of NOAA or any of its subagencies. Lamont-Doherty Earth Observatory contribution number 5745.

REFERENCES

Ackley, S. F., and E. T. Holt, Sea ice data buoys in the Weddell Sea, *CRREL Rep.* 84-11, 18 pp., 1984.

Akitomo, K., T. Awaji, and N. Imasato, Open-ocean convection in the Weddell Sea: Two-dimensional numerical experiments with a nonhydrostatic model, *Deep-Sea Res., 42*, 53-73, 1995.

Alverson, K., and W. B. Owens, Topographic preconditioning of open-ocean deep convection, *J. Phys. Oceanogr., 26(10),* 2196-2213, 1996.

Andreas, E. L., and K. J. Claffey, Air-ice drag coefficients in the western Weddell Sea, 1, values deduced from profile measurements, *J. Geophys. Res., 100(C3),* 4821-4831, 1995.

Bagriantsev, N., A. Gordon, and B. Huber, Weddell Gyre: Temperature maximum stratum, *J. Geophys. Res., 94*, 8331-8334, 1989.

Barber, M., and D. Crane, Current flow in the north-west Weddell Sea, *Antarctic Science, 7,* 39-50, 1995.

Bersch, M., G. Becker, H. Frey, and K. Koltermann, Topographic effects of the Maud Rise on the stratification and circulation of the Weddell Gyre, *Deep-Sea Res., 39,* 303-331, 1992.

Carmack, E. C., A quantitative characterization of water masses in the Weddell Sea during summer, *Deep-Sea Res., 21*, 431-443, 1974.

Carmack, E .C., Water Characteristics of the Southern Ocean south of the Polar Front, in *A Voyage of Discovery*, edited by M. Angel, pp 15-37, Pergamon Press, 1982.

Carmack E. C., and T. D. Foster, On the flow of water out of the Weddell Sea, *Deep-Sea Res., 22*, 711-724, 1975a.

Carmack, E. C., and T. D. Foster, Circulation and distribution of oceanographic properties near the Filchner Ice Shelf, *Deep-Sea Res., 22*, 77-90, 1975b.

Carmack, E. C., and P. D. Killworth, Formation and interleaving of abyssal water masses off Wilkes Land, Antarctica, *Deep-Sea Res., 25,* 357-369, 1978.

Comiso, J. C., and A. L. Gordon, Interannual Variability in Summer Sea Ice Minimum, Coastal Polynyas, and Bottom Water Formation in the Weddell Sea, in *Antarctic Sea Ice Physical Processes, Interactions and Variability, Antarct. Res. Ser.* vol. 74, edited by M. Jeffries, AGU, Washington, D.C., 1998.

Deacon, G. E. R., The hydrology of the Southern Ocean, *Discovery Reports, 15,* 1-124, 1937.

Deacon, G. E. R., The Weddell gyre, *Deep-Sea Res., 26*, 981-995, 1979.

Fahrbach, E., G. Rohardt, and G. Krause, The Antarctic coastal current in the southeast Weddell Sea, *Polar Biology, 12*, 171-182, 1992.

Fahrbach, E., G. Rohardt, M. Schroder, and V. Strass, Transport and structure of the Weddell gyre, *Ann. Geophysics, 12*, 840-855, 1994a.

Fahrbach, E, R. Peterson, G. Rohardt, P. Schlosser, and R. Bayer, Suppression of bottom water formation in the southeastern Weddell Sea, *Deep-Sea Res., 41(2),* 389-411, 1994b.

Fahrbach, E., G. Rohardt, N. Scheele, M. Schroder, V. Strass, and A. Wisotzki, Formation and discharge of deep and bottom water in the northwestern Weddell Sea, *J. Mar. Res., 53(4),* 515-538, 1995.

Fahrbach, E., M. Schröder, and A. Klepikov, Circulation and water masses in the Weddell Sea, *in Physics of Ice-Covered Seas*, Lecture Notes from a Summer School in Savonlinna, Finland 6-17 June, 1994, Helsinki University Press, 1998.

Foldvik, A., T. Kvinge, and T. Torresen, Bottom currents near the continental shelf break in the Weddell Sea, in *Antarct. Res. Ser.* vol. 43, edited by S.S. Jacobs, pp. 21-34, AGU, Washington, D.C., 1985a.

Foldvik, A., T. Gammelsrød, and T. Torresen, Circulation and water masses on the southern Weddell Sea shelf, in *Oceanology of the Antarctic Continental Shelf, Antarct. Res. Ser.* vol. 43, edited by S.S. Jacobs, pp. 5-20, AGU, Washington, D.C., 1985b.

Foster, T. D., and E. C. Carmack, Frontal zone mixing and Antarctic Bottom Water formation in the southern Weddell Sea, *Deep-Sea Res., 23,* 301-317, 1976a.

Foster, T. D., and E. C. Carmack, Temperature and salinity structure in the Weddell Sea, *J. Phys. Oceanogr., 6*, 36-44, 1976b.

Foster, T. D., and J. H. Middleton, Bottom water formation in the western Weddell Sea, *Deep-Sea Res., 26*, 743-762, 1979.

Foster, T. D., and J. H. Middleton, The oceanographic structure of the eastern Scotia Sea - I. Physical Oceanography, *Deep-Sea Res., 31(5),* 529-550, 1984.

Foster, T. D., A. Foldvik, and J. H. Middleton, Mixing and bottom water formation in the shelf break region of the southern Weddell Sea, *Deep-Sea Res., 34,* 1771-1794, 1987.

Frew, R., K. Heywood, and P. Dennis, Oxygen isotope study of water masses in the Princess Elizabeth Trough, Antarctica. *Marine Chemistry, 49,* 141-153, 1995.

Gammelsrød, T., A. Foldvik, O. A. Nost, O. Skagseth, L. G. Anderson, E. Fogelqvist, K. Olsson, T. Tanhua, E. P. Jones, and S. Osterhus, Distribution of Water Masses on the continental Shelf in the Southern Weddell Sea, in *The Polar Oceans and their Role in shaping the global environment, Geophysical Monograph 85*, edited by O. M. Johannessen, R. D. Muench, and J. E. Overland, pp. 109-136, AGU, Washington, D.C., 1994.

Gill, A., Circulation and bottom water production in the Weddell Sea, *Deep-Sea Res., 20(2),* 111- 140, 1973.

Gloersen P., W. Campbell, D. Cavalieri, J. Comiso, C. Parkinson, and H. J. Zwally, Arctic and Antarctic Sea Ice, 1978-1987: Satellite Passive Microwave, Observations and Analysis, *NASA Spec. Publ.* 511, 290 pp., 1992.

Gordon, A. L., General Ocean Circulation, Symposium, Durham, New Hampshire, Oct. 17-20, 1972 pp. 39-53, *Nat. Acad. Sci. Press*, 1975.

Gordon, A. L., Seasonality of Southern Ocean Sea Ice, *Geophys. Res., 85(C5),* 4193-4197, 1981.

Gordon, A. L., Weddell deep water variability, *J. Mar. Res., 40,* 199-217, 1982.

Gordon, A. L., The Southern Ocean - its involvement in

global change, in *Proc. Conf. on Role of the Polar Regions in Global Change*, edited by G. Weller, pp. 249-255, Univ. of Alaska, Fairbanks, 1991.

Gordon, A. L., and P. Tchernia, Waters off Adelie Coast, *in Antarctic Oceanology II: The Australian-New Zealand Sector, Antarctic Research Series* , vol. 19, edited by D. E. Hayes, pp. 59-69, AGU, Washington, D. C., 1972.

Gordon, A. L., and B. A. Huber, Southern Ocean winter mixed layer, *J. Geophys. Res., 95(C7),* 11655-11672, 1990.

Gordon, A. L., B. Huber, H. Hellmer, and A. Ffield, Deep and Bottom Water of the Weddell Sea's Western Rim, *Science, 262,* 95-97, 1993.

Gordon, A. L., and B. A. Huber, Warm Weddell Deep Water west of Maud Rise, *J. Geophys. Res., 100(C7),* 13747-13753, 1995.

Gouretski, V., and A. Danilov, Weddell Gyre: structure of the eastern boundary, *Deep-Sea Res., 40(3),* 561-582, 1993.

Heywood, K. J., R .A. Locarnini, R. D. Frew, P. F. Dennis, and B. A. King, Transport and Water Masses of the Antarctic Slope Front System in the Eastern Weddell Sea, this volume.

Huber, B. A., P. A. Mele, W. E. Haines, A. L. Gordon, and V. I. Lukin, Ice Station Weddell - 1, CTD/Hydrographic Data, Lamont-Doherty Earth Observatory, Palisades, N.Y., Tech Rept LDEO 94-2, 1994.

ISW Group, Ice Station Weddell 1 Explores the Western Edge of the Weddell Sea, *Eos, 74(11),* 121, 124-126, 1993.

Jacobs, S. S., On the nature and significance of the Antarctic Slope Front, *Marine Chemistry, 35,* 9-24, 1991.

Jacobs, S. S., R. G. Fairbanks, and Y. Horibe, Origin and evolution of water masses near the Antarctic continental margin: Evidence from $H_2{}^{18}O/H_2{}^{16}O$ ratio in seawater, in *Oceanology of Antarctic Continental Shelf, Antarct. Res. Ser.* vol. 43, edited by S. S. Jacobs, pp 59-85, AGU, Washington, D.C., 1985.

Killworth, P. D., Mixing on the Weddell Sea continental slope, *Deep-Sea Res., 24,* 427-448, 1977.

Klepikov, V. V., Warm deep waters in the Weddell Sea, in *Soviet Antarctic Expedition 2*, pp.194-198, Elsevier, 1964.

LaBrecque, J. L., and M. E. Ghidella, Estimates of bathymetry, depth to magnetic basement, and sediment thickness for the western Weddell Basin, *Ant. J. of the United States, 27,* 68-70, 1993.

Levine, M. D., L. Padman, R. D. Muench, and J. H. Morison, Internal waves and tides in the western Weddell Sea: Observations from Ice Station Weddell, *J. Geophys. Res., 102(C1),* 1073-1089, 1997.

Locarnini, R. A., Water masses and circulation in the Ross Gyre and environs, PhD. Dissertation, Texas A&M, 87 pp., Dec 1994.

Locarnini, R. A., T. Whitworth, and W.D. Nowlin, The importance of the Scotia Sea on the outflow of Weddell Sea Deep Water, *J. Mar. Res., 51,* 135-153, 1993.

Lytle, V. I., and S. F. Ackley, Heat flux through sea ice in the Western Weddell Sea: Convective and conductive transfer processes, *J. Geophys. Res., 101(C4),* 8853-8868, 1996.

Martinson D. G., Evolution of the southern ocean winter mixed layer and sea-ice: Open deep water formation and ventilation, *J. Geophys. Res., 95,* 11641-11654, 1990.

McDougall, T. J., Thermobaricity, cabbeling, and water-mass conversion, *J. Geophys. Res., 92(C5),* 5448-5464, 1987.

McPhee, M., and D. Martinson, Turbulent mixing under drifting pack ice in the Weddell Sea, *Science, 263,* 219-220, 1994.

McPhee, M., S. Ackley, P. Guest, B. Huber, D. Martinson, J. Morison, R. Muench, L. Padman, and T. Stanton, The Antarctic zone flux experiment, *Bull. Amer. Meteor. Soc. 77,* 1221-1232, 1996.

Mensch, M., R. Bayer, J. Bullister, P. Schlosser, and R. Weiss, The distribution of tritium and CFCs in the Weddell Sea during the mid-1980s, *Progress in Oceanog., 38,* 377-415, 1996.

Mensch, M., W. Smethie, P. Schlosser, R. Weppernig, and R. Bayer, Transient tracer observations during the drift and recovery of Ice Station Weddell, this volume.

Muench, R. D., Relict convective features in the Weddell Sea, In *Deep convection and deep water formation in the oceans,* edited by P.C. Chu and J. C. Gascard, pp. 53-67, Elsevier, Amsterdam, 1991.

Muench, R., H. Fernando, and G. Stegen, Temperature and salinity staircases in the northwestern Weddell Sea, *J. Phys. Oceanogr., 20(2),* 295-306, 1990a.

Muench, R. D., J. T. Gunn, and D. M. Husby, The Weddell-Scotia Confluence in midwinter, *J. Geophys. Res., 95,* 18177-18190, 1990b.

Muench, R. D., B. A. Huber, J. T. Gunn, D. M. Husby, and D. G. Mountain, The Weddell-Scotia marginal ice zone: Physical oceanographic conditions, geographical and seasonal variability, *J. Mar. Systems, 3,* 169-182, 1992.

Muench, R. D., and A. L. Gordon, Circulation and transport of water along the western Weddell Sea margin, *J. Geophs. Res., 100(C9),* 18503-18515, 1995.

Nunes-Vas, R. A., and G. W. Lennon, Physical oceanography of the Prydz Bay region of Antarctic waters, *Deep-Sea Res., 43(5),* 603-641, 1996.

Olbers, D., V. Guretski, G. Seiss, and J. Schroter, Hydrographic Atlas of the Southern Ocean, 82 pp., Bremerhaven, Alfred-Wegener Institute, 1992.

Orsi, A. H., W. D. Nowlin, and T. Whitworth, On the circulation and stratification of the Weddell Gyre, *Deep-Sea Res., 40,* 169-203, 1993.

Orsi, A. H., T. Whitworth, and W. D. Nowlin, On the meridional extent and fronts of the Antarctic Circumpolar Current, *Deep-Sea Research, 42(5),* 641-673, 1995.

Patterson, S. L., and H. A. Sievers, The Weddell-Scotia Confluence, *J. Phys. Oceanog., 10,* 1584-1610, 1980.

Rintoul, S., On the origin and influence of Adelie Land Bottom Water, this volume.

Robertson, R. A., L. Padman, and M. D. Levine, Fine structure, microstructure and vertical mixing in the upper ocean in the western Weddell Sea, *J. Geophys. Res. 100,* 18517-18536, 1995.

Robertson, R. A., L. Padman, and G. Egbert, Tides in the Weddell Sea, this volume.

Schenke, H. W., H. Hinze, F. Niederjasper, T. Schöne, B.

Hoppmann, and S. Dijkstra, The New Bathymetric Charts of the Weddell Sea: AWI BCWS, this volume.

Schlosser, P., R. Bayer, A. Foldvik, T. Gammelsrød, G. Rohardt, and K. Münnich, Oxygen-18 and helium as tracers of Ice Shelf Water and water/ice interaction in the Weddell Sea, *J. Geophys. Res. 95,* 3253-3263, 1990.

Schwerdtfeger, W., The effect of the Antarctic Peninsula on the temperature regime of the Weddell Sea, *Month. Weather Rev., 103 (1),* 45-51, 1975.

Speer, K. G., and A. Forbes, A deep western boundary current in the South Indian Basin, *Deep-Sea Res., 41(9),* 1994.

Tchernia, P., and P. F. Jeannin, Quelques aspects de la circulation Antarctique reveles par l'observation de la derive d'icebergs (1972-83), 92 pp., Paris: Musee National D'Histoire Naturelle, 93 pp., 1983.

Weppernig, R., P. Schlosser, S. Khatiwala, and R.G. Fairbanks, Isotope data from Ice Station Weddell: Implications for deep water formation in the Weddell Sea, *J. Geophys. Res., 101(C11),* 25,723-25,740, 1996.

Whitworth, T., W. Nowlin, A. Orsi, R. Locarnini, and S. Smith, Weddell Sea shelf water in the Bransfield Strait and the Weddell-Scotia Confluence, *Deep-Sea Res., 41,* 629-641, 1994.

Arnold L. Gordon, Lamont-Doherty Earth Observatory of Columbia University, Palisades, N.Y. 10964 (e-mail: agordon@ldeo.columbia.edu)

(Received January 27, 1997; accepted October 4, 1997)